Role of the 't Hooft interaction in the calculation of the mixing angles of the $\eta(547)$ and $\eta'(958)$ mesons

C. M. Shakin* and Huangsheng Wang
Department of Physics and Center for Nuclear Theory, Brooklyn College of the City University of New York, Brooklyn, New York 11210
(Received 30 August 2001; published 12 April 2002)

Recent work has shown that the singlet-octet mixing angles of the $\eta(547)$ and $\eta'(958)$ are different. That may be demonstrated either in extended chiral perturbation theory or by analysis of a large body of experimental data. The conclusion is that the $\eta(547)$ is almost entirely of octet character, while the $\eta'(958)$ is mainly of singlet character with about 10% octet component. It is possible to calculate the mixing angles and decay constants in our generalized Nambu–Jona-Lasinio (NJL) model, which includes a covariant model of confinement. Our model is able to give a good account of the mass values of the $\eta(547)$, $\eta'(958)$, $\eta(1295)$, and $\eta(1440)$ mesons. (We also provide predictions for the mass values of a large number of radially excited states.) It is well known that the $U_A(1)$ symmetry is broken, so that we only have eight pseudo Goldstone bosons, rather than the nine we would have otherwise. In the NJL model that feature may be introduced by including the 't Hooft interaction in the Lagrangian. That interaction reduces the energy of the octet state somewhat and significantly increases the energy of the singlet state, making it possible to fit the mass values of the $\eta(547)$ and $\eta'(958)$ in the NJL model when the 't Hooft interaction is included. In this work, we derive the equations of a covariant random phase approximation that may be used to study the nonet of pseudoscalar mesons. We demonstrate that a consistent treatment of the 't Hooft interaction leads to excellent results for the singlet-octet mixing angles. (The values obtained for the singlet and octet decay constants are also quite satisfactory.) It may be seen that the difference between the up (or down) constituent quark mass and the strange quark mass induces singlet-octet mixing that is too large. However, the 't Hooft interaction contains singlet-octet coupling that enters into the theory with a sign opposite to that of the term arising from the difference of the quark mass values, leading to quite satisfactory results. In this work we present the wave function amplitudes for a number of states of the eta mesons. (The inclusion of pseudoscalar–axial-vector coupling is important for our analysis and results in the need to specify eight wave function amplitudes for each state of the eta mesons.) We present the values of the various constants that parametrize our generalized NJL model and which give satisfactory values of the eta meson masses, decay constants, and mixing angles. It is found that the calculated mass values for the $\eta(1295)$ and $\eta(1440)$ are quite insensitive to variation of the parameters of the model whose values have largely been fixed in our earlier studies of other light mesons.

DOI: 10.1103/PhysRevD.65.094003 PACS number(s): 14.40.Aq, 12.39.Fe

I. INTRODUCTION

The description of η-η' mixing has attracted a good deal of attention over the years. There is a large body of work in which it is assumed that only a single mixing angle may be used [1–6]. Recently, an extended form of chiral perturbation theory has been developed which is based upon the idea that at large n_c the η' becomes a ninth Goldstone boson and an expansion in $1/n_c$ becomes useful [7,8]. Other closely related theoretical methods have also been developed [9,10]. The theoretical analysis clearly shows that two mixing angles are required. There is also a body of work which shows that the analysis of experimental data requires two mixing angles [11–14].

For the moment, we may limit our discussion to a consideration of the properties of the $\eta(547)$ and $\eta'(958)$. There are four fundamental singlet and octet decay constants, which we denote as $\tilde{f}_\eta^{(0)}$, $\tilde{f}_\eta^{(8)}$, $\tilde{f}_{\eta'}^{(0)}$ and $\tilde{f}_{\eta'}^{(8)}$. Rather than quote values for these constants, various mixing schemes provide alternative parametrizations. For example, we may write

$$|\eta\rangle = \cos\theta_\eta |\eta_8\rangle - \sin\theta_\eta |\eta_0\rangle, \tag{1.1}$$

$$|\eta'\rangle = \sin\theta_{\eta'} |\eta_8\rangle + \cos\theta_{\eta'} |\eta_0\rangle, \tag{1.2}$$

and introduce decay constants for the states $|\eta_8\rangle$ and $|\eta_0\rangle$ such that

$$\tilde{f}_\eta^{(8)} = F_8 \cos\theta_\eta, \tag{1.3}$$

$$\tilde{f}_\eta^{(0)} = -F_0 \sin\theta_\eta, \tag{1.4}$$

$$\tilde{f}_{\eta'}^{(8)} = F_8 \sin\theta_{\eta'}, \tag{1.5}$$

and

$$\tilde{f}_{\eta'}^{(0)} = F_0 \cos\theta_{\eta'}. \tag{1.6}$$

One possible point of view is that the mixing angle is energy dependent leading to $\theta_\eta \neq \theta_{\eta'}$ [12]. Another parametrization used by Leutwyler [7], Kaiser and Leutwyler [8], and others is

$$\tilde{f}_\eta^{(8)} = \hat{F}_8 \cos\theta_8, \tag{1.7}$$

*Electronic address: CASBC@CUNYVM.CUNY.EDU

$$\tilde{f}_{\eta}^{(0)} = -\hat{F}_0 \sin\theta_0 , \tag{1.8}$$

$$\tilde{f}_{\eta'}^{(8)} = \hat{F}_8 \sin\theta_8 , \tag{1.9}$$

and

$$\tilde{f}_{\eta'}^{(0)} = \hat{F}_0 \cos\theta_0 . \tag{1.10}$$

We may relate these representations using the equations

$$\tan\theta_8 = \frac{\sin\theta_{\eta'}}{\cos\theta_{\eta}}, \tag{1.11}$$

$$\tan\theta_0 = \frac{\sin\theta_{\eta}}{\cos\theta_{\eta'}}, \tag{1.12}$$

$$\hat{F}_0 = F_0\sqrt{\sin^2\theta_{\eta} + \cos^2\theta_{\eta'}} , \tag{1.13}$$

and

$$\hat{F}_8 = F_8\sqrt{\sin^2\theta_{\eta'} + \cos^2\theta_{\eta}} . \tag{1.14}$$

There is a problem in our use of Eqs. (1.1) and (1.2), since we have calculated orthogonal states $|\eta\rangle$ and $|\eta'\rangle$. Then, if we assume that the states $|\eta_0\rangle$ and $|\eta_8\rangle$ are the same in Eqs. (1.1) and (1.2), we obtain a contradiction if $\theta_\eta \neq \theta_{\eta'}$, since then $\langle\eta|\eta'\rangle = \sin(\theta_\eta - \theta_\eta')$. Therefore, the relations of Eqs. (1.7)–(1.10) are to be preferred when we make use of our model. However, we can discard Eqs. (1.1) and (1.2) and use Eqs. (1.3)–(1.6) and Eqs. (1.7)–(1.10) as alternative representations of the four fundamental quantities $\tilde{f}_{\eta}^{(8)}$, $\tilde{f}_{\eta}^{(0)}$, $\tilde{f}_{\eta'}^{(8)}$, and $\tilde{f}_{\eta'}^{(0)}$, which appear on the left-hand sides of Eqs. (1.3)–(1.6) and Eqs. (1.7)–(1.10). We may then use Eqs. (1.11)–(1.14) to pass between the two representations of the four fundamental decay constants.

In this work we will calculate the mixing angles of the η and η'. It is clear that any theoretical description of the η' wave function requires a model of confinement. Therefore, we will use an extended version of the Nambu–Jona-Lasinio (NJL) model that we have generalized to include a covariant model of confinement. This model and various applications have been described in a number of publications [15–20].

In our model the constituent quark masses are parameters. Ideally, we should solve the Bethe-Salpeter equation along with the Schwinger-Dyson equation. In our Euclidean-space calculation [21], we could solve the one-body (Hartree) aspect of the problem at the same time as the two-body aspect (Bethe-Salpeter equation) and demonstrate that our model exhibits chiral symmetry. At present, we do not know how to make a corresponding calculation in Minkowski space, if we include our model of confinement. However, our model has many useful applications as may be seen in earlier and in the present work.

The Lagrangian of our model is

$$\begin{aligned}\mathcal{L} = {} & \bar{q}(i\partial\!\!\!/ - m^0)q + \frac{G_S}{2}\sum_{i=0}^{8}[(\bar{q}\lambda^i q)^2 + (\bar{q}i\gamma_5\lambda^i q)^2] \\ & - \frac{G_V}{2}\sum_{i=0}^{8}[(\bar{q}\gamma^\mu\lambda^i q)^2 + (\bar{q}\gamma^\mu\gamma_5\lambda^i q)^2] \\ & + \frac{G_D}{2}\{\det[\bar{q}(1+\gamma_5)q] + \det[\bar{q}(1-\gamma_5)q]\} + \mathcal{L}_{\rm tensor} \\ & + \mathcal{L}_{\rm conf} ,\end{aligned} \tag{1.15}$$

Here, the fourth term is the 't Hooft interaction, $\mathcal{L}_{\rm tensor}$ denotes interactions added to study tensor mesons [16], while $\mathcal{L}_{\rm conf}$ denotes our model of confinement. In Eq. (1.15) m^0 is the current quark mass matrix $m^0 = {\rm diag}(m_u^0, m_d^0, m_s^0)$, the λ_i $(i = 1,...,8)$ are the Gell-Mann matrices, and $\lambda_0 = \sqrt{2/3}\mathbb{I}$, with $\mathbb{I}$ being the unit matrix in flavor space. For the Minkowski-space calculations reported here, and in our earlier work, we found it useful to neglect energy transfer by the confining field in the meson rest frame. For example, if we start with the potential $V^C(r) = \kappa r \exp[-\mu r]$ and form the Fourier transform, we have the form of the interaction used in the meson rest frame:

$$V^C(\vec{k} - \vec{k}') = -8\pi\kappa\left[\frac{1}{[(\vec{k} - \vec{k}')^2 + \mu^2]^2} - \frac{4\mu^2}{[(\vec{k}' - \vec{k}')^2 + \mu^2]^3}\right]. \tag{1.16}$$

Here μ is a small parameter used to soften the infrared singularities of V^C. If μ is small enough, the potential approximates a linear potential with "string tension" κ over the range of r relevant for our problem. (Since we use Lorentz-vector confinement, our value of κ differs from that usually quoted for a Lorentz-scalar model of confinement.) The potential of Eq. (1.16) may be put in a covariant form, if we use the four-vectors $\hat{k}^\mu$ and $\hat{k}'^\mu$,

$$\hat{k}^\mu = k^\mu - \frac{(k\cdot P)P^\mu}{P^2}, \tag{1.17}$$

and

$$\hat{k}'^\mu = k'^\mu - \frac{(k'\cdot p)P^\mu}{P^2}, \tag{1.18}$$

since, when $\vec{P} = 0$, we have $\hat{k}^\mu = [0,\vec{k}]$ and $\hat{k}'^\mu = [0,\vec{k}']$.

The parameters of the Lagrangian may be fixed in the study of various light mesons. For example, we may obtain values for G_V and κ in a study of the vector mesons ρ and ω. Including the $\phi(1020)$ in our study leads to a value of the constituent mass of the strange quark. In the present work, we fix the values of G_S and G_D by studying the properties of the η mesons.

We do not attempt to derive our Lagrangian from first principles, although the form of the 't Hooft interaction may be obtained from the study of instanton dynamics in QCD. It

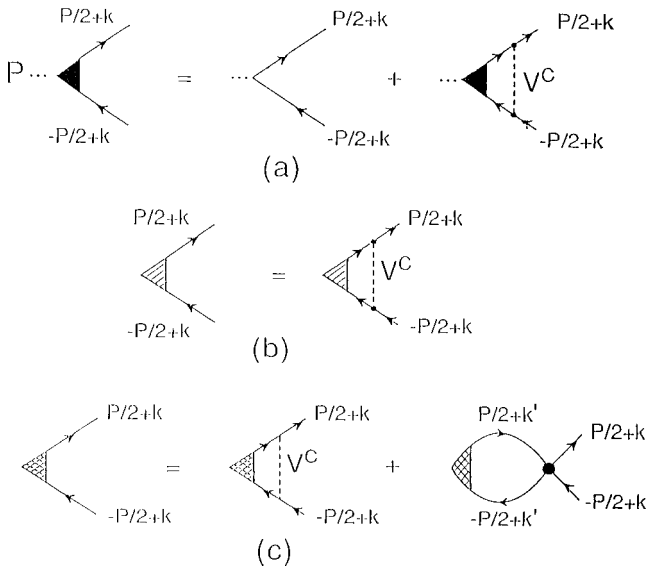

FIG. 1. (a) Schematic representation of the equation for the confinement vertex. Here V^C denotes the confining field. (b) The homogeneous version of the equation shown in (a). (c) A representation of the homogeneous equation for the vertex $\hat{\Gamma}$ that includes the effects of both confinement and the short-range NJL interaction.

is worth noting that, when calculating the effective coupling constants in the singlet, octet, and mixed channels (G_{00}, G_{88}, and G_{08}) in the study of pseudoscalar mesons, the value of G_S in each channel is modified by a term proportional to the product of G_D and various quark vacuum condensates. (See Sec. X.) Since G_S is of order $1/n_c$ and G_D is of order $(1/n_c)^3$, the correction term is of order $(1/n_c)^2$. That is, G_S is modified at the next order in $1/n_c$ when calculating G_{00}, G_{88}, and G_{08}.

While it may be possible to derive the full Lagrangian including the term proportional to G_S from the study of instanton dynamics, that has not been done. For the purposes of this work we use the SU(3)-flavor version of the NJL model that has been used by many researchers. The utility of our Lagrangian lies in its application in studies of the full range of light mesons, with a fixed parameter set. (An attempt to derive our Lagrangian from QCD is beyond the scope of our paper.)

It is useful to obtain the wave functions of various mesons by first calculating vertex functions. It is possible to define several vertex functions in the study of pseudoscalar mesons. We may define functions that correspond to the use of only the confining interaction, as in Figs. 1(a) and 1(b). Here the vertex functions were denoted as $\overline{\Gamma}_5(P,k)$ and $\overline{\Gamma}^{\mu}_L(P,k)$, where the latter function was needed when we studied pseudoscalar–axial-vector mixing [17]. Note that, when we wish to construct wave functions, we solve the homogeneous equation of Fig. 1(b) rather than the inhomogeneous equation of Fig. 1(a). In the present work we will solve the homogeneous equation that is given in a schematic representation in Fig. 1(c). In this case we include the NJL interaction, or the NJL interaction plus the confining interaction. The resulting vertex functions will be denoted as $\overline{\Gamma}_P(P,k)$ and $\overline{\Gamma}^{\mu}_A(P,k)$.

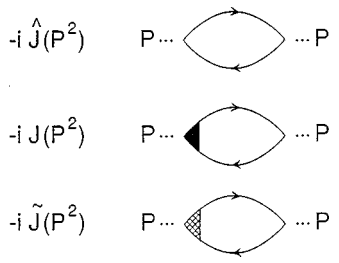

FIG. 2. The three types of polarization functions considered in this work: (a) The function $\hat{J}(P)$, defined in the absence of a confinement model; (b) the function $J(P)$, which includes either of the confinement vertex functions Γ_5^{+-} or Γ_L^{+-} in its definition; (c) the function $\tilde{J}(P)$, defined in terms of either of the vertex functions Γ_P^{+-} or Γ_A^{+-}.

(The bar over the vertex function is a reminder that these functions have a Dirac matrix structure.) These various vertex functions may be used to define a number of vacuum polarization integrals, as seen in Fig. 2. Once these polarization integrals have been defined, it is a relatively simple matter to obtain equations for the vertex functions $\overline{\Gamma}_P(P,k)$ and $\overline{\Gamma}^{\mu}_A(P,k)$.

The organization of our work is as follows. In Sec. II we define various vertex functions that are needed in our study of pesudoscalar mesons. We consider the general case in which the quark and antiquark masses are different, so that the formalism may be used to calculate the properties of the kaon. In Secs. III and IV we introduce a series of vacuum polarization functions. The first set of these functions is defined in the absence of a confinement model. The second set of polarization functions is defined in terms of the vertex that describes the effects of confinement. The third set of these functions is only introduced to facilitate a derivation of the relativistic random phase approximation (RPA) equations which are to be used in this work. (A discussion of nonrelativistic RPA equations, appropriate to the study of particle-hole excitations in nuclei or nuclear matter, may be found in Refs. [22] and [23].) The third set of vacuum polarization functions are functionals of the unknown vertex functions that include the effects of both the NJL interaction and confinement. Alternatively, these polarization functions may be written in terms of the wave functions that are the solutions of the RPA equations that we solve. In Sec. V we present relativistic RPA equations suitable for the study of the pion and the kaon and their radial excitations. We take pseudoscalar–axial-vector coupling into account, since that is an important feature in any study of the pseudoscalar mesons. In Sec. VI we introduce normalized RPA wave functions for the pion and kaon and also provide expressions for the decay constants. In Sec. VII we turn to a consideration of both pseudoscalar–axial-vector coupling and singlet-octet mixing. The resulting wave functions have eight components, since the vertex structure could be proportional to γ_5 or $\gamma_0\gamma_5$ in the meson rest frame and one has both singlet and octet states. Each of these states has a ''large'' and ''small'' component in the sense of the RPA. We present the eight coupled equations needed in our study of the eta mesons in

Sec. VII. In Sec. VIII we present the wave functions of the $\eta(547)$, $\eta'(958)$, $\eta(1295)$, and $\eta(1440)$ mesons and two other states found at 1653 and 1698 MeV. In Sec. IX we introduce normalized wave functions for the eta mesons and provide expressions for the octet and singlet decay constants. In Sec. X we present our results for the various mixing angles and decay constants defined for the $\eta(547)$ and $\eta'(958)$. Finally, Sec. XI contains some further discussion and conclusions.

II. VERTEX FUNCTIONS FOR THE CONFINING INTERACTION

In this section we review various relations that serve to define the vertex functions that satisfy an equation of the form given in Fig. 1(a). We define a pseudoscalar vertex matrix [17]

$$\overline{\Gamma}_{5,ab}(P,k)=\gamma_5-i\int\frac{d^4k'}{(2\pi)^4}[\gamma^\rho S_a(P/2+k')\times\overline{\Gamma}_{5,ab}(P,k')S_b(-P/2+k')\gamma_\rho]\times V^C(\vec{k}-\vec{k}'),\tag{2.1}$$

where $S_a(P/2+k)=[\not P/2+\not k-m_a+i\eta]^{-1}$, etc. We define the functions Γ_5^{+-} and Γ_5^{-+}:

$$\Lambda_a^{(+)}(\vec{k})\overline{\Gamma}_{5,ab}(P,k)\Lambda_b^{(-)}(-\vec{k})=\Gamma_{5,ab}^{+-}(P,k)\Lambda_a^{(+)}(\vec{k})\gamma_5\Lambda_b^{(-)}(-\vec{k}),\tag{2.2}$$

and

$$\Lambda_a^{(-)}(-\vec{k})\overline{\Gamma}_{5,ab}(P,k)\Lambda_b^{(+)}(\vec{k})=\Gamma_{5,ab}^{-+}(P,k)\Lambda_a^{(-)}(-\vec{k})\gamma_5\Lambda_b^{(+)}(\vec{k}),\tag{2.3}$$

where

$$\Lambda_a^{(+)}(\vec{k})=\frac{\not k_a+m_a}{2m_a}\tag{2.4}$$

and

$$\Lambda_b^{(-)}(-\vec{k})=\frac{\tilde{\not k}_b+m_b}{2m_b}.\tag{2.5}$$

Here, $k_a^\mu=[E_a(\vec{k}),\vec{k}]$ and $\tilde{k}_b^\mu=[-E_b(\vec{k}),\vec{k}]$.

We also define a longitudinal matrix vertex [17]

$$\overline{\Gamma}_{L,ab}^\mu(P,k)=\frac{P^\mu\not P}{P^2}\gamma_5-i\int\frac{d^4k'}{(2\pi)^4}\gamma^\rho S_a(P/2+k')\times\overline{\Gamma}_{L,ab}^\mu(P,k')S_b(-P/2+k')\gamma_\rho V^C(\vec{k}-\vec{k}')\tag{2.6}$$

and introduce the function $\Gamma_{L,ab}^{+-}(P,k)$:

$$\Lambda_a^{(+)}(\vec{k})\vec{\Gamma}_{L,ab}^\mu(P,k)\Lambda_b^{(-)}(-\vec{k})=\frac{P^\mu}{\sqrt{P^2}}\Gamma_{L,ab}^{+-}(P,k)\Lambda_a^{(+)}(\vec{k})\gamma_5\Lambda_b^{(-)}(-\vec{k}).\tag{2.7}$$

There is a corresponding equation defining $\overline{\Gamma}_{L,ab}^{-+}(P,k)$. It is useful to write

$$\overline{\Gamma}_{L,ab}^\mu(P,k)=\frac{P^\mu}{\sqrt{P^2}}\overline{\Gamma}_{L,ab}(P,k),\tag{2.8}$$

so that Eq. (2.7) becomes

$$\Lambda_a^{(+)}(\vec{k})\overline{\Gamma}_{L,ab}(P,k)\Lambda_b^{(-)}(-\vec{k})=\Gamma_{L,ab}^{+-}(P,k)\Lambda_a^{(+)}(\vec{k})\gamma_5\Lambda_b^{(-)}(-\vec{k}),\tag{2.9}$$

etc. We find that

$$\Gamma_{L,ab}^{+-}(P,k)=\left(\frac{m_bE_a(\vec{k})+m_aE_b(\vec{k})}{m_am_b+E_a(\vec{k})E_b(\vec{k})+\vec{k}^2}\right)-\int\frac{d^3k'}{(2\pi)^3}\frac{(m_am_b)^2}{4E_a(\vec{k}')E_b(\vec{k}')}\times\frac{V^C(\vec{k}-\vec{k}')}{m_am_b+E_a(\vec{k})E_b(\vec{k})+\vec{k}^2}\times C(\vec{k},\vec{k}')\frac{\Gamma_{L,ab}^{+-}(P,k')}{P^0-E_a(\vec{k}')-E_b(\vec{k}')}\tag{2.10}$$

with

$$C(\vec{k},\vec{k}')=\frac{1}{m_a^2m_b^2}\{m_b^2[E_a(\vec{k})E_a(\vec{k}')-\vec{k}\cdot\vec{k}']+m_a^2[E_b(\vec{k})E_b(\vec{k}')-\vec{k}\cdot\vec{k}']+2m_am_b[-E_a(\vec{k})E_b(\vec{k})-\vec{k}^2-E_a(\vec{k}')E_b(\vec{k}')-\vec{k}'^2+\tfrac{1}{2}E_a(\vec{k})E_b(\vec{k}')+\vec{k}\cdot\vec{k}'+\tfrac{1}{2}E_a(\vec{k}')E_b(\vec{k})]-2[E_a(\vec{k})E_b(\vec{k})+\vec{k}^2][E_a(\vec{k}')E_b(\vec{k}')+\vec{k}'^2]-2m_a^2m_b^2\}.\tag{2.11}$$

We also have

$$\Gamma^{-+}_{L,ab}(P,k)=-\left(\frac{m_bE_a(\vec{k})+m_aE_b(\vec{k})}{m_am_b+E_a(\vec{k})E_b(\vec{k})+\vec{k}^2}\right)+\int\frac{d^3k'}{(2\pi)^3}\frac{(m_am_b)^2}{4E_a(\vec{k})E_b(\vec{k}')}\frac{V^C(\vec{k}-\vec{k}')}{m_am_b+E_a(\vec{k})E_b(\vec{k})+\vec{k}^2}$$
$$\times C(\vec{k},\vec{k}')\frac{\Gamma^{-+}_{L,ab}(P,k')}{P^0+E_a(\vec{k}')+E_b(\vec{k}')}. \tag{2.12}$$

[In Eqs. (2.10) and (2.12) we have corrected a misprint that appeared in Ref. [17].] We note the relation $\Gamma^{-+}_{L,ab}(-P^0,|\vec{k}|)=-\Gamma^{+-}_{L,ab}(P^0,|\vec{k}|)$. The functions $\Gamma^{+-}_{5,ab}(P,k)$ and $\Gamma^{-+}_{5,ab}(P,k)$ satisfy equations similar to Eqs. (2.10)–(2.12), except that the inhomogeneous terms are both equal to unity [17]. Therefore, we have $\Gamma^{-+}_{5,ab}(-P^0,|\vec{k}|)=\Gamma^{+-}_{5,ab}(P^0,|\vec{k}|)$.

These vertex functions may be used to define various vacuum polarization functions that are free of the singularities that would appear in a theory without confinement when the quark and antiquark go on mass shell. (See Fig. 2.) We describe various polarization functions in the next section.

III. VACUUM POLARIZATION FUNCTIONS

We start with a definition of the polarization functions in the absence of confinement [17]

$$-i\hat{J}^{PP}_{ab}(P)=(-1)2n_c\mathrm{Tr}\int\frac{d^4k}{(2\pi)^4}\times[i\gamma_5 iS_a(P/2+k)i\gamma_5 iS_b(-P/2+k)], \tag{3.1}$$

$$-i\hat{J}^{PA}_{\mu,ab}(P)=(-1)2n_c\mathrm{Tr}\int\frac{d^4k}{(2\pi)^4}\times[iS_a(P/2+k)i\gamma_5 iS_b(-P/2+k)\gamma_\mu\gamma_5], \tag{3.2}$$

$$-i\hat{J}^{AP}_{\mu,ab}(P)=(-1)2n_c\mathrm{Tr}\int\frac{d^4k}{(2\pi)^4}\times[iS_a(P/2+k)\gamma_\mu\gamma_5 iS_b(-P/2+k)i\gamma_5], \tag{3.3}$$

and

$$-i\hat{J}^{AA}_{\mu\nu,ab}(P)=(-1)2n_c\mathrm{Tr}\int\frac{d^4k}{(2\pi)^4}\times[iS_a(P/2+k)\gamma_\mu\gamma_5 iS_b(-P/2+k)\gamma_\nu\gamma_5]. \tag{3.4}$$

Here $n_c=3$ is the number of colors. We also define [17]

$$\hat{J}^{PA}_{\mu,ab}(P)=iJ^{PA}_{ab}(P^2)\frac{P_\mu}{\sqrt{P^2}}, \tag{3.5}$$

$$\hat{J}^{AP}_{\mu,ab}(P)=iJ^{AP}_{ab}(P^2)\frac{P_\mu}{\sqrt{P^2}}, \tag{3.6}$$

and

$$\hat{J}^{AA}_{\mu\nu,ab}(P)=-\tilde{g}_{\mu\nu}(P)\hat{J}^{AA}_{T,ab}(P^2)-\frac{P_\mu P_\nu}{P^2}\hat{J}^{AA}_{L,ab}(P^2), \tag{3.7}$$

with $\tilde{g}_{\mu\nu}=g_{\mu\nu}-P_\mu P_\nu/P^2$. Note also that $\hat{J}^{AP}(P^2)=-\hat{J}^{PA}(P^2)$ and $P_\mu\tilde{g}^{\mu\nu}=\tilde{g}^{\mu\nu}P_\nu=0$.

We now include the confinement vertex in the definitions of the polarization integrals. We define

$$-iJ^{PP}_{ab}(P^2)=(-1)2n_c\int\frac{d^4k}{(2\pi)^4}\mathrm{Tr}[i\gamma_5 iS_a(P/2+k)\times i\bar{\Gamma}_{5,ab}(P,k)iS_b(-P/2+k)]. \tag{3.8}$$

We find, with $\vec{P}=0$,

$$J^{PP}_{ab}(P^2)=-2n_c\int\frac{d^3k}{(2\pi)^3}\frac{[E_a(\vec{k})E_b(\vec{k})+\vec{k}^2+m_am_b]}{E_a(\vec{k})E_b(\vec{k})}\times\left[\frac{\Gamma^{+-}_{5,ab}(P^0,|\vec{k}|)}{P^0-E_a(\vec{k})-E_b(\vec{k})}-\frac{\Gamma^{-+}_{5,ab}(-P^0,|\vec{k}|)}{P^0+E_a(\vec{k})+E_b(\vec{k})}\right], \tag{3.9}$$

which may be written as

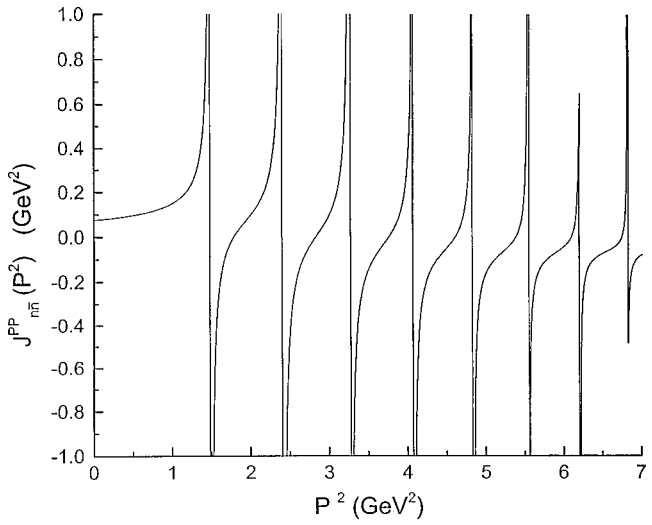

FIG. 3. The function $J^{PP}_{nn}(P^2)$. Here $\kappa=0.055\ \mathrm{GeV}^2$ and $m_u=0.364$ GeV.

$$J^{PP}_{ab}(P^2)=-2n_c\int\frac{d^3k}{(2\pi)^3}\frac{[E_a(\vec{k})E_b(\vec{k})+\vec{k}^2+m_am_b]}{E_a(\vec{k})E_b(\vec{k})}\times\Gamma^{+-}_{5,ab}(P^0,|\vec{k}|)\left[\frac{1}{P^0-E_a(\vec{k})-E_b(\vec{k})}-\frac{1}{P^0+E_a(\vec{k})+E_b(\vec{k})}\right]. \tag{3.10}$$

Values obtained for $J^{PP}_{nn}(P^2)$ and $J^{PP}_{s\bar{s}}(P^2)$ are shown in Figs. 3 and 4. (A Gaussian regulator of the form $\exp[-\vec{k}^2/\alpha^2]$, with $\alpha=0.605$ GeV, was used when calculating these functions.)

We now define

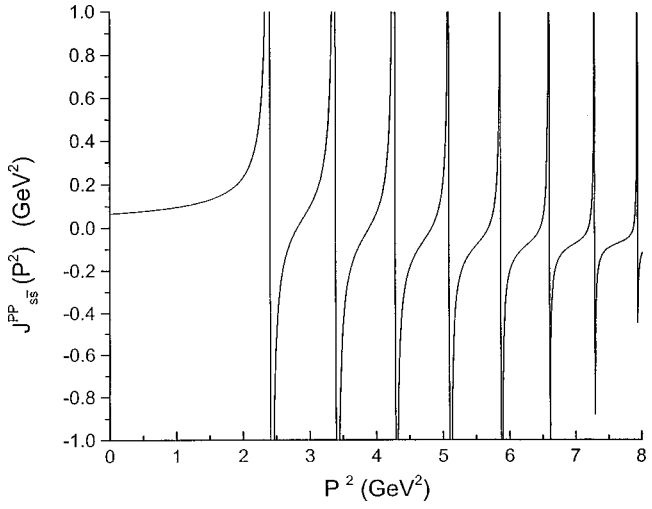

FIG. 4. The function $J^{PP}_{s\bar{s}}(P^2)$. Here $\kappa=0.055\ \mathrm{GeV}^2$ and $m_s=0.565$ GeV.

$$-iJ^{PA}_{ab}(P^2)=(-1)2n_c\int\frac{d^4k}{(2\pi)^4}\mathrm{Tr}[iS_a(P/2+k)\times i\bar{\Gamma}_5(P,k)iS_b(-P/2+k)\gamma_0\gamma_5] \tag{3.11}$$

and

$$-iJ^{AP}_{\mu,ab}(P^2)=(-1)2n_c\int\frac{d^4k}{(2\pi)^4}\mathrm{Tr}[iS_a(P/2+k)\times i\bar{\Gamma}_{L,\mu}(P,k)iS_b(-P/2+k)i\gamma_5]. \tag{3.12}$$

We use Eqs. (2.8) and (2.9) to find

$$J^{PA}_{ab}(P^2)=-2n_c\int\frac{d^3k}{(2\pi)^3}\frac{[m_aE_b(\vec{k})+m_bE_a(\vec{k})]}{E_a(\vec{k})E_b(\vec{k})}\times\left[\frac{\Gamma^{+-}_{5,ab}(P^0,|\vec{k}|)}{P^0-E_a(\vec{k})-E_b(\vec{k})}+\frac{\Gamma^{-+}_{5,ab}(-P^0,|\vec{k}|)}{P^0+E_a(\vec{k})+E_b(\vec{k})}\right]. \tag{3.13}$$

Using the relation $\Gamma^{-+}_{5,ab}(-P^0,|\vec{k}|)=\Gamma^{+-}_{5,ab}(P^0,|\vec{k}|)$, the last relation may be written

$$J^{PA}_{ab}(P^2)=-2n_c\int\frac{d^3k}{(2\pi)^3}\frac{[m_b(\vec{k})E_a(\vec{k})+m_aE_b(\vec{k})]}{E_a(\vec{k})E_b(\vec{k})}\times\Gamma^{+-}_{5,ab}(P^0,|\vec{k}|)\left[\frac{1}{P^0-E_a(\vec{k})-E_b(\vec{k})}+\frac{1}{P^0+E_a(\vec{k})+E_b(\vec{k})}\right]. \tag{3.14}$$

We note that $J^{PA}_{ab}(0)=0$.

In a similar fashion, we find

$$J^{AP}_{ab}(P^2)=2n_c\int\frac{d^3k}{(2\pi)^3}\frac{[m_am_b+\vec{k}^2+E_a(\vec{k})E_b(\vec{k})]}{E_a(\vec{k})E_b(\vec{k})}\times\Gamma^{+-}_{L,ab}(P^0,|\vec{k}|)\left[\frac{1}{P^0-E_a(\vec{k})-E_b(\vec{k})}+\frac{1}{P^0+E_a(\vec{k})+E_b(\vec{k})}\right] \tag{3.15}$$

and

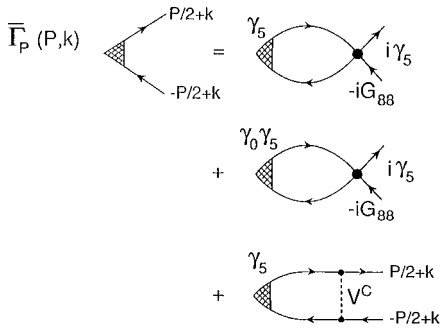

FIG. 5. A schematic representation of the equation for $\overline{\Gamma}_P(P,k)$.

$$J_{ab}^{AA}(P^2)=2n_c\int\frac{d^3k}{(2\pi)^3}\frac{[m_bE_a(\vec{k})+m_aE_b(\vec{k})]}{E_a(\vec{k})E_b(\vec{k})}\times\Gamma_{L,ab}^{+-}(P^0,|\vec{k}|)\left[\frac{1}{P^0-E_a(\vec{k})-E_b(\vec{k})}-\frac{1}{P^0+E_a(\vec{k})+E_b(\vec{k})}\right],\tag{3.16}$$

where we have used the relation $\Gamma_L^{-+}(-P^0,|\vec{k}|)=-\Gamma_L^{+-}(P^0,|\vec{k}|)$. Relations such as those given in Eqs. (3.5)–(3.7) may also be written for the functions $J_\mu^{PA}(P)$, $J_\mu^{AP}(P)$, and $J_{\mu\nu}^{AA}(P)$.

IV. VERTEX FUNCTIONS FOR THE SUM OF THE NJL AND THE CONFINING INTERACTIONS

We now include the NJL interaction in addition to the confining interaction in the equation for the vertex functions, as in Figs. 5 and 6. We define a new set of polarization intergrals by replacing $\Gamma_{5,ab}^{+-}(P^0,|\vec{k}|)$ by $\Gamma_{P,ab}^{+-}(P^0,|\vec{k}|)$ and $\Gamma_{L,ab}^{+-}(P^0,|\vec{k}|)$ by $\Gamma_{A,ab}^{+-}(P^0,|\vec{k}|)$, etc., in the expressions given in Sec. III. With this procedure we obtain the vacuum polarization functions appearing in Fig. 2(c). We denote these new polarization functions as $\tilde{J}^{PP},\tilde{J}^{PA},\tilde{J}^{AA}$, etc. Thus,

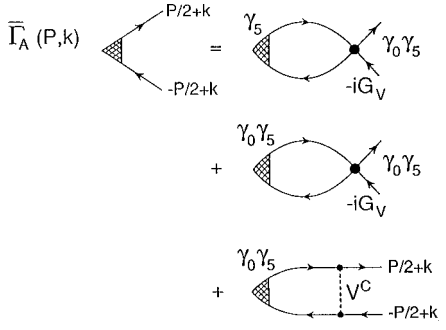

FIG. 6. A schematic representation of the equation for $\overline{\Gamma}_A(P,k)$.

$$\tilde{J}_{ab}^{PP}(P^2)=-2n_c\int\frac{d^3k}{(2\pi)^3}\frac{[E_a(\vec{k})E_b(\vec{k})+\vec{k}^2+m_am_b]}{E_a(\vec{k})E_b(\vec{k})}\times\Gamma_{P,ab}^{+-}(P^0,|\vec{k}|)\left[\frac{1}{P^0-E_a(\vec{k})-E_b(\vec{k})}-\frac{1}{P^0+E_a(\vec{k})+E_b(\vec{k})}\right]\tag{4.1}$$

$$=-2n_c\int\frac{d^3k}{(2\pi)^3}\frac{[E_a(\vec{k})E_b(\vec{k})+\vec{k}^2+m_am_b]}{E_a(\vec{k})E_b(\vec{k})}\times[\tilde{\phi}_P^+(P^0,|\vec{k}|)+\tilde{\phi}_P^-(P^0,|\vec{k}|)],\tag{4.2}$$

where we have defined

$$\tilde{\phi}_P^+(P^0,|\vec{k}|)=\frac{\Gamma_{P,ab}^{+-}(P^0,|\vec{k}|)}{P^0-E_a(\vec{k})-E_b(\vec{k})}\tag{4.3}$$

and

$$\tilde{\phi}_P^-(P^0,|\vec{k}|)=-\frac{\Gamma_{P,ab}^{-+}(-P^0,|\vec{k}|)}{P^0+E_a(\vec{k})+E_b(\vec{k})},$$

$$=-\frac{\Gamma_{P,ab}^{+-}(P^0,|\vec{k}|)}{P^0+E_a(\vec{k})+E_b(\vec{k})}.\tag{4.4}$$

Since we will be dealing with bound-state wave functions, we will write $\tilde{\phi}_P^+(P_i^0,|\vec{k}|)$ as $\tilde{\phi}_{P,i}^+(k)$ and $\tilde{\phi}_P^-(P_i^0,|\vec{k}|)$ as $\tilde{\phi}_{P,i}^-(k)$, where $k=|\vec{k}|$.

Similarly, we define $\tilde{J}_{ab}^{PA}(P^2)$ by the replacement of $\Gamma_{5,ab}^{+-}(P^0,|\vec{k}|)$ by $\Gamma_{P,ab}^{+-}(P^0,|\vec{k}|)$, etc. Thus,

$$\tilde{J}_{ab}^{PA}(P^2)=-2n_c\int\frac{d^3k}{(2\pi)^3}\frac{[m_bE_a(\vec{k})+m_aE_b(\vec{k})]}{E_a(\vec{k})E_b(\vec{k})}\times[\tilde{\phi}_{P,i}^+(k)-\tilde{\phi}_{P,i}^-(k)].\tag{4.5}$$

We also have

$$\tilde{J}_{ab}^{AP}(P^2)=2n_c\int\frac{d^3k}{(2\pi)^3}\frac{[m_am_b+\vec{k}^2+E_a(\vec{k})E_b(\vec{k})]}{E_a(\vec{k})E_b(\vec{k})}\times[\tilde{\phi}_{A,i}^+(k)-\tilde{\phi}_{A,i}^-(k)],\tag{4.6}$$

where

$$\tilde{\phi}_{A,i}^+(k)=\frac{\Gamma_{A,ab}^{+-}(P_i^0,|\vec{k}|)}{P_i^0-E_a(\vec{k})-E_b(\vec{k})}\tag{4.7}$$

and

$$\tilde{\phi}^{-}_{A,i}(k)=\frac{\Gamma^{-+}_{A,ab}(-P^0_i,|\vec{k}|)}{P^0_i+E_a(\vec{k})+E_b(\vec{k})}$$

$$=-\frac{\Gamma^{+-}_{A,ab}(P^0_i,|\vec{k}|)}{P^0_i+E_a(\vec{k})+E_b(\vec{k})}. \tag{4.8}$$

With these definitions we may write

$$\tilde{J}^{AA}_{ab}(P^2)=2n_c\int\frac{d^3k}{(2\pi)^3}\frac{[m_bE_a(\vec{k})+m_aE_b(\vec{k})]}{E_a(\vec{k})E_b(\vec{k})}$$
$$\times\Gamma^{+-}_{A,ab}(P^0,|\vec{k}|)\left[\frac{1}{P^0-E_a(\vec{k})-E_b(\vec{k})}\right.$$
$$\left.-\frac{1}{P^0+E_a(\vec{k})+E_b(\vec{k})}\right] \tag{4.9}$$

$$=2n_c\int\frac{d^3k}{(2\pi)^3}\frac{[m_bE_a(\vec{k})+m_aE_b(\vec{k})]}{E_a(\vec{k})E_b(\vec{k})}$$
$$\times[\tilde{\phi}^{+}_{A,i}(k)+\tilde{\phi}^{-}_{A,i}(k)]. \tag{4.10}$$

V. PROPERTIES OF THE PION AND KAON: COUPLED EQUATIONS FOR THE WAVE FUNCTION AMPLITUDES $\phi^+_P(k)$, $\phi^-_P(k)$, $\phi^+_A(k)$, AND $\phi^-_A(k)$

With the array of definitions made in the previous sections, we may easily obtain the coupled equations relating ϕ^+_P, ϕ^-_P, ϕ^+_A, and ϕ^-_A. The equation for the vertex functions in the presence of both the NJL interaction and the confining interaction is indicated in a schematic fashion in Figs. 5 and 6. For the moment, let us consider only the NJL interaction and Fig. 5. In general, we may write $\overline{\Gamma}=\overline{\Gamma}_P+\overline{\Gamma}_A$. Taking matrix elements of $\overline{\Gamma}_P$ between the projectors $\Lambda^{(+)}_a(\vec{k})$ and $\Lambda^{(-)}_b(-\vec{k})$ and canceling a common factor of $\Lambda^{(+)}(\vec{k})\gamma_5\Lambda^{(-)}(-\vec{k})$, we obtain an equation that couples $\Gamma^{+-}_P(P^0,k)$ to $\Gamma^{+-}_A(P^0,k)$:

$$\Gamma^{+-}_P(P^0,k)=e^{-k^2/2\alpha^2}\tilde{J}^{PP}(P^2)G_P-e^{-k^2/2\alpha^2}\tilde{J}^{AP}(P^2)G_P \tag{5.1}$$

$$=-2n_cG_Pe^{-k^2/2\alpha^2}\int\frac{d^3k'}{(2\pi)^3}\frac{F(k')e^{-k'^2/2\alpha^2}}{E_a(k')E_b(k')}$$
$$\times\left[\frac{\Gamma^{+-}_P(P^0_i,k')}{P^0-E_a(k')-E_b(k')}\right.$$
$$\left.-\frac{\Gamma^{+-}_P(P^0_i,k')}{P^0+E_a(k')+E_b(k')}\right]$$
$$-2n_cG_Pe^{-k^2/2\alpha^2}\int\frac{d^3k'}{(2\pi)^3}\frac{F(k')e^{-k'^2/2\alpha^2}}{E_a(k')E_b(k')}$$
$$\times\left[\frac{\Gamma^{+-}_A(P^0_i,k')}{P^0-E_a(k')-E_b(k')}\right.$$
$$\left.+\frac{\Gamma^{+-}_A(P^0_i,k')}{P^0+E_a(k')+E_b(k')}\right]. \tag{5.2}$$

Since the NJL interaction requires regulation we have replaced the coupling constant G_P by $\exp[-k^2/2\alpha^2]\times G_P\exp[-k'^2/2\alpha^2]$. This replacement corresponds to the regularization procedure we used in our earlier work [15–18]. Here, G_P is the interaction to be used when calculating the properties of the pion and kaon. The value of G_P depends upon G_S, G_D, and the value of the quark vacuum condensates [24]. In Eq. (5.1) we have introduced the function

$$F(k)=[E_a(\vec{k})E_b(\vec{k})+\vec{k}^2+m_am_b]. \tag{5.3}$$

We also define

$$G(k)=m_aE_b(\vec{k})+m_bE_a(\vec{k}). \tag{5.4}$$

It is useful to introduce a degree of symmetry in the interaction we will derive by defining

$$\phi^+_{P,i}(k)=\frac{k\sqrt{F(k)}}{\sqrt{2E_a(\vec{k})E_b(\vec{k})}}\tilde{\phi}^+_{P,i}(k), \tag{5.5}$$

and

$$\phi^-_{P,i}(k)=\frac{k\sqrt{F(k)}}{\sqrt{2E_a(\vec{k})E_b(\vec{k})}}\tilde{\phi}^-_{P,i}(k), \tag{5.6}$$

with similar definitions for $\phi^+_A(k)$ and $\phi^-_A(k)$.

Thus Eq. (5.2) may be rewritten, with $k=|\vec{k}|$ and $k'=|\vec{k}'|$, as

$$[P^0_i-E_a(k)-E_b(k)]\phi^+_{P,i}(k)=\int dk'[H^{PP}_N(k,k')\phi^+_{P,i}(k')$$
$$+H^{PP}_N(k,k')\phi^-_{P,i}(k')$$
$$+H^{PA}_N(k,k')\phi^+_{A,i}(k')$$
$$-H^{PA}_N(k,k')\phi^-_{A,i}(k')]. \tag{5.7}$$

Here, $H^{PP}_N(k,k')$ is a symmetric function,

$$H^{PP}_N(k,k')=-\frac{n_c}{\pi^2}\frac{G_{88}kk'\sqrt{F(k)F(k')}e^{-k^2/2\alpha^2}e^{-k'^2/2\alpha^2}}{\sqrt{E_a(k)E_b(k)E_a(k')E_b(k')}}, \tag{5.8}$$

while

$$H_N^{PA}(k,k') = -\frac{n_c}{\pi^2} G_V \sqrt{F(k)F(k')} \times \frac{kk' e^{-k^2/2\alpha^2} e^{-k'^2/2\alpha^2}}{\sqrt{E_a(k)E_b(k)E_a(k')E_b(k')}}, \quad (5.9)$$

and

$$H_N^{AP}(k,k') = -\frac{n_c}{\pi^2} G_{88} \sqrt{F(k)/F(k')} \times \frac{G(k')kk' e^{-k^2/2\alpha^2} e^{-k'^2/2\alpha^2}}{\sqrt{E_a(k)E_b(k)E_a(k')E_b(k')}}. \quad (5.10)$$

We also obtain

$$H_N^{AA}(k,k') = \frac{n_c}{\pi^2} G_V kk' \sqrt{F(k)/F(k')} G(k') \times \frac{e^{-k^2/2\alpha^2} e^{-k'^2/2\alpha^2}}{\sqrt{E_a(k)E_b(k)E_a(k')E_b(k')}}. \quad (5.11)$$

In these equations the exponential factors are the Gaussian regulators. (For our work we have used $\alpha = 0.605$ GeV.)

We may obtain another equation by writing

$$\Gamma_P^{+-}(P^0,k) = -[P^0 + E_a(\vec{k}) + E_b(\vec{k})]\phi_P^-(P^0,k) \quad (5.12)$$

on the left-hand side of Eq. (5.2).

We may also use the relation (see Fig. 6)

$$\overline{\Gamma}_A(P,k) = -e^{-k^2/2\alpha^2} \tilde{J}^{PA}(P^2) G_V \gamma_0 \gamma_5 + e^{-k'^2/2\alpha^2} \tilde{J}^{AA}(P^2) G_V \gamma_0 \gamma_5 \quad (5.13)$$

and form the matrix element between $\Lambda_a^{(+)}(\vec{k})$ and $\Lambda_b^{(-)}(-\vec{k})$. Thus,

$$\Gamma_A^{+-}(P^0,k) = -e^{-k^2/2\alpha^2} \tilde{J}^{PA}(P^2) G_V + e^{-k^2/2\alpha^2} \tilde{J}^{AA}(P^2) G_V. \quad (5.14)$$

Here $\hat{J}^{PP}(P^2)$, $\hat{J}^{PA}(P^2)$, and $\hat{J}^{AA}(P^2)$ differ from the functions defined in Sec. IV, since they include the regulator $\exp[-k'^2/2\alpha^2]$ in the integral defining these functions. If we put

$$\Gamma_A^{+-}(P^0,k) = [P^0 - E_a(\vec{k}) - E_b(\vec{k})]\phi_A^+(P^0,k)$$

or

$$\Gamma_A^{+-}(P^0,k) = -[P^0 + E_a(\vec{k}) + E_b(\vec{k}]\phi_A^-(P^0,k), \quad (5.15)$$

we obtain a total of four equations relating ϕ_P^+, ϕ_P^-, ϕ_A^+, and ϕ_A^-.

Before writing these equations, we consider the confining interaction. Our treatment of the confinement is such that we neglect pair production by the confining field in the meson rest frame so that, if we construct a matrix of the interaction terms, the confining interaction appears only in the diagonal elements. We may identify the contribution of the confining interaction by using the equations satisfied by $\Gamma_5^{+-}(P,k)$ and $\Gamma_L^{+-}(P,k)$ given previously. To that end, it is useful to write

$$C(\vec{k},\vec{k}') = C_0(k,k') + \vec{k}\cdot\vec{k}' C_1(k,k') \quad (5.16)$$

and define

$$V_l^C(k,k') = \frac{1}{2}\int dx\, P_l(x) V^C(\vec{k} - \vec{k}'), \quad (5.17)$$

where $P_l(x)$ is a Legendre function. We find the symmetric interaction

$$H_C(k,k') = -\frac{1}{4\pi^2} \frac{(m_a m_b)^2 kk' \{C_0(k,k')V_0^C(k,k') + kk' C_1(k,k')V_1^C(k,k')\}}{\sqrt{F(k)F(k')}\sqrt{E_a(k)E_b(k)E_a(k')E_b(k')}}. \quad (5.18)$$

Note that the confining interaction does not require regularization.

We may then write the four coupled equations for ϕ_P^+, ϕ_P^-, ϕ_A^+, and ϕ_A^- as

$$\int dk' (\{[E_a(k') + E_b(k')]\delta(k-k') + H_N^{PP}(k,k') + H_C(k,k')\}\phi_{P,i}^+(k') + H_N^{PP}(k,k')\phi_{P,i}^-(k') + H_N^{PA}(k,k')\phi_{A,i}^+(k') - H_N^{PA}(k,k')\tilde{\phi}_{A,i}^-(k')) = P_i^0 \phi_{P,i}^+(k), \quad (5.19)$$

$$\int dk' (-H_N^{PP}(k,k')\phi_{p,i}^+(k') - \{[E_a(k') + E_b(k')]\delta(k-k') + H_N^{PP}(k,k') + H_C(k,k')\}\phi_{P,i}^-(k') - H^{PA}(k,k')\phi_{A,i}^+(k') + H^{PA}(k,k')\phi_{A,i}^-(k'))$$

$$= P_i^0 \phi_{P,i}^-(k), \tag{5.20}$$

$$\int dk' (H_N^{AP}(k,k')\phi_{P,i}^+(k') - H_N^{AP}(k,k')\phi_{P,i}^-(k') + \{[E_a(k')+E_b(k')]\delta(k-k') + H_N^{AA}(k,k') + H_C(k,k')\}\phi_{A,i}^+(k') + H_N^{AA}(k,k')\phi_{A,i}^-(k')) = P_i^0 \phi_{A,i}^+(k), \tag{5.21}$$

and

$$\int dk' (-H_N^{AP}(k,k')\phi_{P,i}^+(k') + H^{AP}(k,k')\phi_{P,i}^-(k') - H_N^{AA}(k,k')\phi_{A,i}^+(k') - \{[E_a(k')+E_b(k')]\delta(k-k') + H_N^{AA}(k,k') + H_C(k,k')\}\phi_{A,i}^-(k')) = P_i^0 \phi_{A,i}^-(k). \tag{5.22}$$

Note that for any solution with $P_i^0 > 0$ there is another solution with the energy $-P_i^0$. If the first solution has a wave function characterized by ϕ_P^+, ϕ_P^-, ϕ_A^+, and ϕ_A^-, the second solution is obtained by the transformation $\phi_P^+ \to \phi_P^-$, $\phi_P^- \to \phi_P^+$, $\phi_A^+ \to -\phi_A^-$, $\phi_A^- \to -\phi_A^+$, and $P_i^0 \to -P_i^0$.

VI. CALCULATION OF NORMALIZED WAVE FUNCTIONS AND PION AND KAON DECAY CONSTANTS

We may define normalized wave functions by multiplying $\phi_P^+(k)$, $\phi_P^-(k)$, $\phi_A^+(k)$, and $\phi_A^-(k)$ by a normalization factor $\sqrt{N_i}$, where

$$\frac{1}{N_i} = \frac{1}{2M_i}\frac{2n_c}{\pi^2}\int dk\{|\phi_{P,i}^+(k)|^2 - |\phi_{P,i}^-(k)|^2\}, \tag{6.1}$$

where M_i is the mass of the meson. Here we have considered the case in which $\phi_A^+(k)$ and $\phi_A^-(k)$ are small and the masses of the quark and antiquark are equal. [The minus sign that appears in Eq. (6.1) is a characteristic of calculations made in the RPA.]

In the case that $\phi_A^+(k)$ and $\phi_A^-(k)$ are significant, the appropriate normalization factor is

$$\frac{1}{N_i} = \frac{1}{2M_i}\frac{2n_c}{\pi^2}\int dk\{|\phi_{P,i}^+(k) + \beta_{ab}(k)\phi_{A,i}^+(k)|^2 - |\phi_{P,i}^-(k) + \beta_{ab}(k)\phi_{A,i}^-(k)|^2\}, \tag{6.2}$$

where

$$\beta_{ab}(k) = \frac{[E_a(k)+m_a][E_b(k)+m_b] - \vec{k}^2}{[E_a(k)+m_a][E_b(k)+m_b] + \vec{k}^2}. \tag{6.3}$$

When $m_a = m_b = m$, $\beta_{ab}(k) = m/E(k)$. We may define

$$\phi_{P,N}^+(k) = \sqrt{N_i}\phi_{P,i}^+(k), \tag{6.4}$$

$$\phi_{P,N}^-(k) = \sqrt{N_i}\phi_{P,i}^-(k), \tag{6.5}$$

etc.

When $m_a \neq m_b$, a calculation of the meson decay constant yields

$$f_{K,i} = \frac{n_c}{\sqrt{2}M_i\pi^2}\int k\,dk\frac{[m_a E_b(k) + m_b E_a(k)]}{\sqrt{E_a(k)E_b(k)F(k)}} \times \sqrt{N_i}\{[\phi_{P,i}^+(k) - \phi_{P,i}^-(k)] + [\phi_{A,i}^+(k) + \phi_{A,i}^-(k)]\}. \tag{6.6}$$

Note that in the chiral limit ($M_i \to 0$) the term in curly brackets also vanishes, such that the decay constant remains finite. Further, in the case $m_a = m_b = m$, we have the simple form

$$f_{\pi,i} = \frac{n_c}{\pi^2 M_i}\int k\,dk\left(\frac{m}{E(k)}\right)\sqrt{N_i} \times \{[\phi_{P,i}^+(k) - \phi_{P,i}^-(k)] + [\phi_{A,i}^+(k) + \phi_{A,i}^-(k)]\}, \tag{6.7}$$

since $F(k) \to 2E^2(k)$ when the quark masses are equal.

VII. WAVE FUNCTIONS FOR PSEUDOSCALAR MESONS WITH SINGLET-OCTET MIXING

We make use of the equations depicted in Figs. 5 and 6. It is again useful to define polarization functions $\tilde{J}^{PP}(P^2)$, $\tilde{J}^{PA}(P^2)$, and $\tilde{J}^{AA}(P^2)$, which have the confinement vertex functions $\Gamma_{5,ab}^{+-}(P^0,k)$ and $\Gamma_{L,ab}^{+-}(P^0,k)$ replaced by $\Gamma_{P,ab}^{+-}(P^0,k)$ and $\Gamma_{A,ab}^{+-}(P^0,k)$. For the study of the η mesons we will need $\Gamma_{P,n\bar{n}}^{+-}(P^0,k)$, $\Gamma_{P,s\bar{s}}^{+-}(P^0,k)$, $\Gamma_{A,n\bar{n}}^{+-}(P^0,k)$, and $\Gamma_{A,s\bar{s}}^{+-}(P^0,k)$. We will also introduce the singlet and octet versions of these functions, $\Gamma_{P,0}^{+-}(P^0,k)$, $\Gamma_{P,8}^{+-}(P^0,k)$, $\Gamma_{A,0}^{+-}(P^0,k)$, and $\Gamma_{A,8}^{+-}(P^0,k)$.

In this work we will pass between the singlet-octet representation and the $n\bar{n}$, $s\bar{s}$ representation. We may use a matrix M to connect these representations:

$$\begin{pmatrix} \lambda_{n\bar{n}} \\ \lambda_{s\bar{s}} \end{pmatrix} = M\begin{pmatrix} \lambda_8/\sqrt{2} \\ \lambda_0/\sqrt{2} \end{pmatrix}. \tag{7.1}$$

Here

$$M = \frac{1}{\sqrt{3}}\begin{pmatrix} 1 & \sqrt{2} \\ -\sqrt{2} & 1 \end{pmatrix}, \tag{7.2}$$

so that

$$\lambda_{n\bar{n}} = \frac{\lambda_8}{\sqrt{6}} + \frac{\lambda_0}{\sqrt{3}} \tag{7.3}$$

and

$$\lambda_{s\bar{s}} = -\frac{\lambda_8}{\sqrt{3}} + \frac{\lambda_0}{\sqrt{6}}. \tag{7.4}$$

We may write a vertex for the η mesons of the form

$$\bar{\Gamma}_\eta(k) = \Gamma^{+-}_{P,n\bar{n}}(k)\,\gamma_5\lambda_{n\bar{n}} + \Gamma^{+-}_{P,s\bar{s}}(k)\,\gamma_5\lambda_{s\bar{s}} + \Gamma^{+-}_{A,n\bar{n}}(k)\,\gamma_0\gamma_5\lambda_{n\bar{n}} + \Gamma^{+-}_{A,s\bar{s}}(k)\,\gamma_0\gamma_5\lambda_{s\bar{s}}, \tag{7.5}$$

where we have anticipated forming the expression $\Lambda^{(+)}(k)\bar{\Gamma}_\eta(k)\Lambda^{(-)}(-\vec{k})$. We also define a series of wave function amplitudes:

$$\phi^+_{P,n\bar{n}}(k) = \frac{k\Gamma^{+-}_{P,n\bar{n}}(k)}{P^0 - 2E_u(k)}, \tag{7.6}$$

$$\phi^-_{P,n\bar{n}}(k) = -\frac{k\Gamma^{+-}_{P,n\bar{n}}(k)}{P^0 + 2E_u(k)}, \tag{7.7}$$

$$\phi^+_{P,s\bar{s}}(k) = \frac{k\Gamma^{+-}_{P,s\bar{s}}(k)}{P^0 - 2E_s(k)}, \tag{7.8}$$

$$\phi^-_{P,s\bar{s}}(k) = -\frac{k\Gamma^{+-}_{P,s\bar{s}}(k)}{P^0 + 2E_s(k)}, \tag{7.9}$$

$$\phi^+_{A,n\bar{n}}(k) = \frac{k\Gamma^{+-}_{A,n\bar{n}}(k)}{P^0 - 2E_u(k)}, \tag{7.10}$$

$$\phi^-_{A,n\bar{n}}(k) = -\frac{k\Gamma^{+-}_{A,n\bar{n}}(k)}{P^0 + 2E_u(k)}, \tag{7.11}$$

$$\phi^+_{A,s\bar{s}}(k) = \frac{k\Gamma^{+-}_{A,s\bar{s}}(k)}{P^0 - 2E_s(k)}, \tag{7.12}$$

and

$$\phi^-_{A,s\bar{s}}(k) = -\frac{k\Gamma^{+-}_{A,s\bar{s}}(k)}{P^0 + 2E_s(k)}. \tag{7.13}$$

Once we have defined these functions, we may introduce $\phi^+_{A,0}(k)$, $\phi^+_{P,8}(k)$, $\phi^-_{P,0}(k)$, $\phi^-_{P,8}(k)$, $\phi^+_{A,0}(k)$, $\phi^+_{A,8}(k)$, $\phi^-_{A,0}(k)$, and $\phi^-_{A,8}(k)$. We choose to solve for the functions in the singlet-octet representation. To that end, we write $E_u(k) = [\vec{k}^2 + m_u^2]^{1/2}$, $E_s(k) = [\vec{k}^2 + m_s^2]^{1/2}$, and define

$$E_{00}(k) = \frac{2}{\sqrt{3}}[2E_u(k) + E_s(k)], \tag{7.14}$$

$$E_{88}(k) = \frac{2}{\sqrt{3}}[E_u(k) + 2E_s(k)], \tag{7.15}$$

and

$$E_{08}(k) = \frac{2\sqrt{3}}{3}[E_u(k) - E_s(k)], \tag{7.16}$$

with $E_{80}(k) = E_{08}(k)$.

We then need to solve the following eight equations, with the functions $H^{PP}_{ij}(k,k')$, $H^{PA}_{ij}(k,k')$, $H^{AP}_{ij}(k,k')$, $H^{AA}_{ij}(k,k')$, $H^{PP(C)}_{ij}(k,k')$, and $H^{AA(C)}_{ij}(k,k')$ defined in the Appendix. (Here, i and j are each either 0 or 8.) The equations are

$$\begin{aligned}\int dk' \{ & [E_{00}(k)\,\delta(k-k') + G_{00}H^{PP}_{00}(k,k') + H^{PP(C)}_{00}(k,k')]\phi^+_{P,0}(k') \\ & + [E_{08}(k)\,\delta(k-k') + G_{08}H^{PP}_{88}(k,k')]\phi^+_{P,8}(k') + G_{00}H^{PP}_{00}(k,k')\phi^-_{P,0}(k') \\ & + G_{08}H^{PP}_{88}(k,k')\phi^-_{P,8}(k') - G_{00}H^{PA}_{00}(k,k')\phi^+_{A,0}(k') - G_{08}H^{PA}_{88}(k,k')\phi^+_{A,8}(k') \\ & + G_{00}H^{PA}_{00}(k,k')\phi^-_{A,0}(k') + G_{08}H^{PA}_{88}(k,k')\phi^-_{A,0}(k)\} = P^0\phi^+_{P,0}(k),\end{aligned} \tag{7.17}$$

$$\begin{aligned}\int dk' \{ & [G_{80}H^{PP}_{00}(k,k') + E_{80}(k)\,\delta(k-k')]\phi^+_{P,0}(k') + [E_{88}(k)\,\delta(k-k') + G_{88}H^{PP}_{88}(k,k') \\ & + H^{PP(C)}_{88}(k,k')]\phi^+_{P,8}(k') + [G_{80}H^{PP}_{00}(k,k')]\phi^-_{P,0}(k') + G_{88}H^{PP}_{88}(k,k')\phi^-_{P,8}(k') \\ & - G_{80}H^{PA}_{00}(k,k')\phi^+_{A,0}(k') - G_{88}H^{PA}_{88}(k,k')\phi^+_{A,8}(k') + G_{80}H^{PA}_{00}(k,k')\phi^-_{A,0}(k') \\ & + G_{88}H^{PA}_{88}(k,k')\phi^-_{A,8}(k')\} = P^0\phi^+_{P,8}(k),\end{aligned} \tag{7.18}$$

$$\int dk'\{-G_{00}H_{00}^{PP}(k,k')\phi_{P,0}^{+}(k')-G_{08}H_{88}^{PP}(k,k')\phi_{P,8}^{+}(k')$$
$$-[E_{00}(k)\delta(k-k')+G_{00}H_{00}^{PP}(k,k')+H_{00}^{PP(C)}(k,k')]\phi_{P,0}^{-}(k')-[E_{08}(k)\delta(k-k')$$
$$+G_{08}H_{88}^{PP}(k,k')]\phi_{P,8}^{-}(k')+G_{00}H_{00}^{PA}(k,k')\phi_{A,0}^{+}(k')+G_{08}H_{88}^{PA}(k,k')\phi_{A,8}^{+}(k')$$
$$-G_{00}H_{00}^{PA}(k,k')\phi_{A,0}^{-}(k')-G_{08}H_{88}^{PA}(k,k')\phi_{A,8}^{-}(k')\}=P^0\phi_{P,0}^{-}(k), \tag{7.19}$$

$$\int dk'\{-G_{80}H_{00}^{PP}(k,k')\phi_{P,0}^{+}(k')-G_{88}H_{88}^{PP}(k,k')\phi_{P,8}^{+}(k')$$
$$-G_{80}H_{00}^{PP}(k,k')\phi_{P,0}^{-}(k')-[E_{88}(k)\delta(k-k')+G_{88}H_{88}^{PP}(k,k')$$
$$+H_{88}^{PP(C)}(k,k')]\phi_{P,8}^{-}(k')+G_{80}H_{00}^{PA}(k,k')\phi_{A,0}^{+}(k')+G_{88}H_{88}^{PA}(k,k')\phi_{A,8}^{+}(k')$$
$$-G_{80}H_{00}^{PA}(k,k')\phi_{A,0}^{-}(k')-G_{88}H_{88}^{PA}(k,k')\phi_{A,8}^{-}(k')\}=P^0\phi_{P,8}^{-}(k), \tag{7.20}$$

$$\int dk'\{-G_V H_{00}^{AP}(k,k')\phi_{P,0}^{+}(k')+G_V H_{00}^{AP}(k,k')\phi_{P,0}^{-}(k')+[E_{00}\delta(k-k')$$
$$+G_V H_{00}^{AA}(k,k')+H_{00}^{AA(C)}(k,k')]\phi_{A,0}^{+}(k')+[E_{08}(k)\delta(k-k')+G_V H_{08}^{AA}(k,k')]\phi_{A,8}^{+}(k')$$
$$+G_V H_{00}^{AA}(k,k')\phi_{A,0}^{-}(k')+G_V H_{08}^{AA}(k,k')\phi_{A,8}^{-}(k')\}=P^0\phi_{A,0}^{+}(k), \tag{7.21}$$

$$\int dk'\{-G_V H_{88}^{AP}(k,k')\phi_{P,8}^{+}(k')+G_V H_{88}^{AP}(k,k')\phi_{P,8}^{-}(k')+[E_{80}\delta(k-k')$$
$$+G_V H_{80}^{AA}(k,k')]\phi_{A,0}^{+}(k')+[E_{88}(k)\delta(k-k')+G_V H_{88}^{AA}(k,k')+H_{88}^{AA(C)}(k,k')]\phi_{A,8}^{+}(k')$$
$$+G_V H_{80}^{AA}(k,k')\phi_{A,0}^{-}(k')+G_V H_{88}^{AA}(k,k')\phi_{A,8}^{-}(k')\}=P^0\phi_{A,8}^{+}(k), \tag{7.22}$$

$$\int dk'\{G_V H_{00}^{AP}(k,k')\phi_{P,0}^{+}(k')-G_V H_{00}^{AP}(k,k')\phi_{P,0}^{-}(k')-G_V H_{00}^{AA}(k,k')\phi_{A,0}^{+}(k')$$
$$-G_V H_{08}^{AA}(k,k')\phi_{A,8}^{+}(k')-[E_{00}(k)\delta(k-k')+G_V H_{00}^{AA}(k,k')+H_{00}^{AA(C)}(k,k')]\phi_{A,0}^{-}(k')$$
$$-[E_{08}(k)\delta(k-k')-G_V H_{08}^{AA}(k,k')]\phi_{A,8}^{-}(k')\}=P^0\phi_{A,0}^{-}(k), \tag{7.23}$$

and

$$\int dk'\{G_V H_{88}^{AP}(k,k')\phi_{P,8}^{+}(k')-G_V H_{88}^{AP}(k,k')\phi_{P,8}^{-}(k')-G_V H_{80}^{AA}(k,k')\phi_{A,0}^{+}(k')$$
$$-G_V H_{88}^{AA}(k,k')\phi_{A,8}^{+}(k')-[E_{80}(k)\delta(k-k')+G_V H_{80}^{AA}(k,k')]\phi_{A,0}^{-}(k')$$
$$-[E_{88}(k)\delta(k-k')+G_V H_{88}^{AA}(k,k')+H_{88}^{AA(C)}(k,k')]\phi_{A,8}^{-}(k')\}=P^0\phi_{A,8}^{-}(k). \tag{7.24}$$

VIII. WAVE FUNCTIONS FOR THE $\eta(547)$ AND $\eta'(958)$ AND THEIR RADIAL EXCITATIONS

The energies of states bound in the confining field are shown in Fig. 7. The first column gives the energies of the $n\bar{n}$ states (1.216, 1.550, 1.811, 2.015, 2.200, 2.359, 2.489, 2.610, and 2.712 GeV), while the third column gives the energies of the $s\bar{s}$ states (1.559, 1.838, 2.072, 2.258, 2.423, 2.573, and 2.698 GeV). The two cross-hatched regions indicate the continuum of the model for the $n\bar{n}$ and $s\bar{s}$ states, respectively. (For example, for the $n\bar{n}$ states, the continuum threshold is $E_{n\bar{n}}^{\rm cont}=2m_u+\kappa/\mu e=2.751$ GeV.) Each of the states in columns one and three is doubly degenerate, with a wave function associated with either a γ_5 or a $\gamma_0\gamma_5$ vertex in the meson rest frame.

The second column shows the results obtained upon the diagonalization of the RPA Hamiltonian. (Here we show only the positive-energy states.) The arrows give some indication of how various states are distributed into the levels of col-

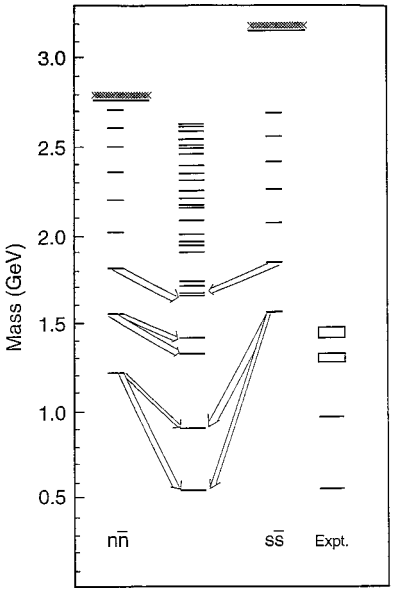

FIG. 7. The first and third columns of levels show the $n\bar{n}$ and $s\bar{s}$ states bound in the confining field, respectively. The second column shows the 28 levels found when the RPA Hamiltonian is brought into diagonal form. The various arrows show the parentage of the resulting states. The $\eta(547)$ has about 75% of the $1\ ^1S_0\ n\bar{n}$ state that has the γ_5 vertex and about 25% of the $1\ ^1S_0\ s\bar{s}$ state that has the γ_5 vertex. These percentages are reversed for the $\eta'(958)$. The $1\ ^1S_0\ n\bar{n}$ and $s\bar{s}$ states with the $\gamma_0\gamma_5$ vertex are fragmented over many states. The $\eta(1295)$ and $\eta(1440)$ are almost entirely of $2\ ^1S_0\ n\bar{n}$ character.

umn 2. The $1\ ^3S_0\ n\bar{n}$ state bound in the confining field that has a γ_5 vertex is found with about 75% probability in the lowest state of column 2 and with about 25% probability in the next excitation. The two lowest energy states in column 2 represent the $\eta(547)$ and $\eta'(958)$. The distribution of the

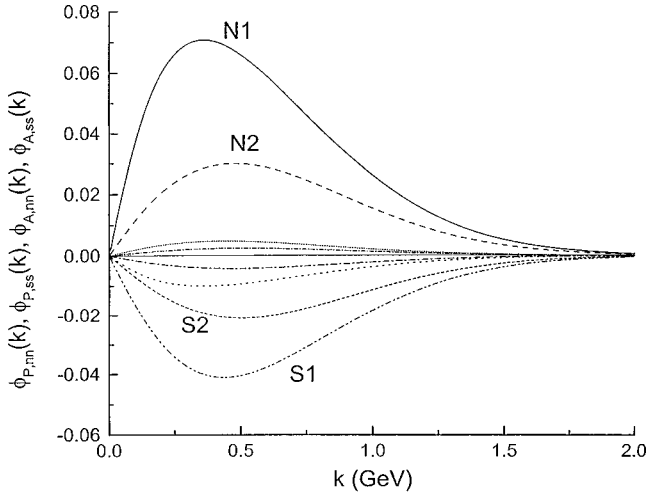

FIG. 8. The wave function for the $\eta(547)$ found at 555 MeV. The various components are $\phi^+_{P,n\bar{n}}(k)$ (solid, $N1$), $\phi^-_{P,n\bar{n}}(k)$ (dash, $N2$), $\phi^+_{A,n\bar{n}}(k)$ (dot, $N3$), $\phi^-_{A,n\bar{n}}(k)$ (dash dot, $N4$), $\phi^+_{P,s\bar{s}}(k)$ (dash dot dot, $S1$), $\phi^-_{P,s\bar{s}}(k)$ (short dash, $S2$), $\phi^+_{A,s\bar{s}}(k)$ (short dot, $S3$), and $\phi^-_{A,s\bar{s}}(k)$ (short dash dot, $S4$).

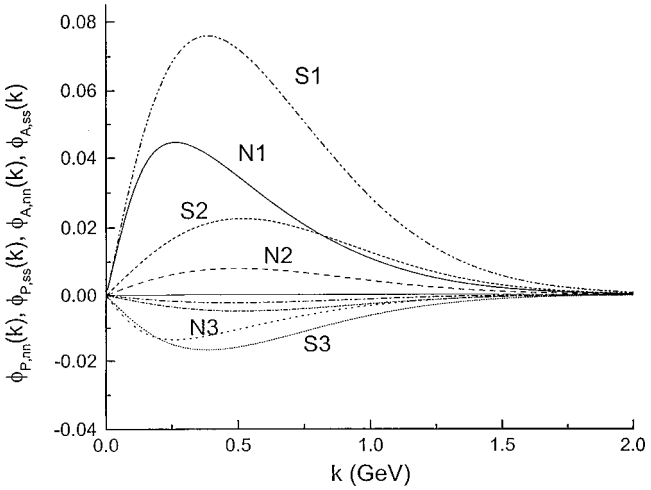

FIG. 9. The wave function of the $\eta'(958)$ found at 949 MeV. (Symbols the same in Fig. 8.)

$1\ ^3S_0\ s\bar{s}$ state has 21% probability in the $\eta(547)$ and 79% in the $\eta(958)$. The $n\bar{n}$ and $s\bar{s}\ 1\ ^3S_0$ states bound in the confining field that have the $\gamma_0\gamma_5$ vertex are highly fragmented over many of the states in column 2. The wave functions $\phi^+_{P,n\bar{n}}(k)$, $\phi^-_{P,n\bar{n}}(k)$, $\phi^+_{A,n\bar{n}}(k)$,..., etc., for the $\eta(547)$ are shown in Fig. 8. Here, $\phi^-_{P,n\bar{n}}(k)$ $(N2)$ and $\phi^-_{P,s\bar{s}}(k)$ $(S2)$ are rather large in a state with a relatively small mass such as the $\eta(547)$. The wave function of the $\eta(547)$ has dominant components $\phi^+_{P,n\bar{n}}(k)$ $(N1)$ and $\phi^+_{P,s\bar{s}}(k)$ $(S1)$.

In Fig. 9 we show the wave function of the $\eta'(958)$ which we find at 949 MeV. Here $\phi^+_{P,s\bar{s}}(k)$ $(S1)$ and $\phi^+_{P,n\bar{n}}(k)$ $(N1)$ are the dominant components. In Figs. 8 and 9 we also see a small amplitude for the $1\ ^3S_0\ \phi^+_{A,s\bar{s}}(k)$ $(N3)$ component, which we stated had a rather fragmented distribution. In Fig. 10 we show the $\eta(1295)$, which we find at 1319 MeV. (See Table I.) This state is dominated by the $2\ ^3S_0\ n\bar{n}$ state, with the component $\phi^+_{A,n\bar{n}}(k)$ $(N3)$ larger than $\phi^+_{P,n\bar{n}}(k)$ $(N1)$. We see that the ''small components'' are indeed small for the more massive mesons.

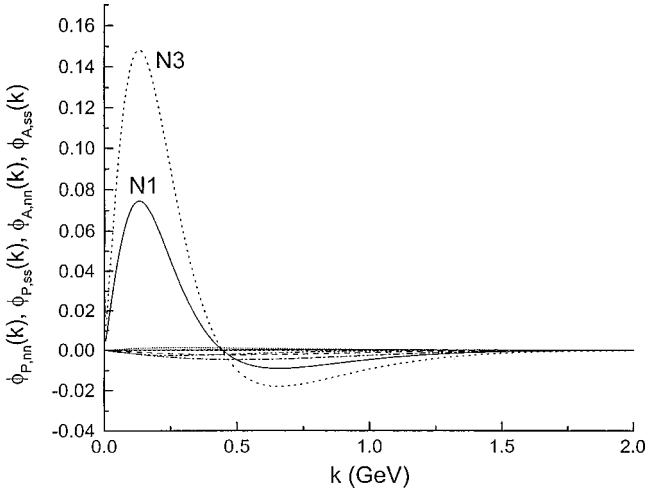

FIG. 10. The wave function of the $\eta(1295)$ found at 1319 MeV. (Symbols the same as in Fig. 8.)

TABLE I. Results of numerical calculation using the parameter sets given in Table II. Here we have used $\kappa=0.55$ GeV^2 and $\mu=0.010$ GeV. The various angles and decay constants were defined in the Introduction. The values for θ_0, θ_8, $\hat{F}_0$, and $\hat{F}_8$ were obtained using Eqs. (1.11)–(1.14) and the values given in Ref. [12] for θ_η, $\theta_{\eta'}$, F_0, and F_8, which are reproduced in the table. If one fixes F_8 at the chiral perturbation theory value of $1.28 f_\pi = 169$ MeV, the values given in Ref. [12] for a fit to experimental data are $\theta_\eta = (-6.9 \pm 2.1)°$, $\theta_{\eta'} = (-24.6 \pm 2.3)°$, and $F_0 = (1.34 \pm 0.07) f_\pi = 177 \pm 9$ MeV. When fitting experimental data for the $\eta\gamma$ and $\eta'\gamma$ transition form factors, Feldman and Kroll [13] find $\theta_8 = 22.2°$, $\theta_0 = -9.1°$, and $\hat{F}^{(0)}/f_\pi = 1.20$ after fixing $\hat{F}^{(8)}/f_\pi = 1.28$.

	Ref. [12]	Set I	Set II	Set III	Set IV
$m_\eta(547)$ (MeV)	—	538	536	527	555
$m_{\eta'}(958)$ (MeV)	—	911	942	963	949
$m_\eta(1295)$ (MeV)	—	1319	1318	1317	1319
$m_\eta(1440)$ (MeV)	—	1414	1416	1419	1411
$\tilde{f}_\eta^{(8)}$ (MeV)	—	177.2	178.6	180.9	163
$\tilde{f}_\eta^{(0)}$ (MeV)	—	27.59	24.51	18.95	52.8
$\tilde{f}_{\eta'}^{(8)}$ (MeV)	—	−84.26	−84.64	−80.97	−105
$\tilde{f}_{\eta'}^{(8)}$ (MeV)	—	159.2	157.3	156.0	150
F_8 (MeV)	$(1.32 \pm 0.06) f_\pi = 174 \pm 8$ MeV	179.3	180.3	181.9	170
F_0 (MeV)	$(1.37 \pm 0.07) f_\pi = 181 \pm 9$ MeV	180.3	178.2	174.2	190
θ_η	$(-5.7 \pm 2.7)°$	−8.81°	−7.82°	−6.26°	−16.1°
$\theta_{\eta'}$	$(-24.6 \pm 2.3)°$	−28.0°	−28.0°	−26.4°	−38.2°
θ_0	$(-7.0 \pm 2.7)°$	−9.83°	−8.76°	−6.94°	−19.4°
θ_8	$(-21.5 \pm 2.4)°$	−25.4°	−25.4°	−24.1°	−32.8°
$\theta_0 - \theta_8$	16.4° Ref. [10]	15.6°	16.6°	17.2°	13.4°
$\hat{F}_0$ (MeV)	$(1.21 \pm 0.07) f_\pi = 160 \pm 9$ MeV	161	159	157	158
$\hat{F}_8$ (MeV)	188 ± 11	196	198	198	194
G_D (GeV^{-5})	—	−180	−200	−220	−161.6 ($G_{08}=0$)

In Fig. 11 we show the wave function of the $\eta(1440)$, which we find at 1411 MeV. Here the state is almost entirely the $2\ ^3S_0\ n\bar{n}$ state that has the γ_5 vertex $(N1)$. In Fig. 12 we show the wave function of the state at 1653 MeV. Here the $n\bar{n}$ components account for 96% of the norm, with $\phi^+_{A,n\bar{n}}(k)$ $(N3)$ larger than $\phi^+_{P,n\bar{n}}(k)$ $(N1)$. These components arise from the $3\ ^3S_0\ n\bar{n}$ state bound in the confining field, as indicated in Fig. 7. In Fig. 13 we show the wave functions of the state found at 1698 MeV. Here the $2\ ^3S_0\ s\bar{s}$ states play an important role, with $\phi^+_{A,s\bar{s}}(k)$ $(N3)$ being the dominant component. (See Fig. 7.)

On the right-hand side of Fig. 7 we show the experimentally observed states: $\eta(547)$, $\eta'(958)$, $\eta(1295)$, and $\eta(1440)$. These are in good correspondence with the four lowest energy states of our model.

IX. NORMALIZATION OF WAVE FUNCTIONS AND CALCULATION OF DECAY CONSTANTS

We may define a normalization factor for each state of mass M_i:

$$\frac{1}{N_i} = \frac{n_c}{2\pi^2 M_i} \int dk \Bigg\{ \Bigg[\Bigg(\phi^+_{P,n\bar{n}}(k) + \frac{m_u}{E_u(k)} \phi^+_{A,n\bar{n}}(k) \Bigg)^2 - \Bigg(\phi^-_{P,n\bar{n}}(k) + \frac{m_u}{E_u(k)} \phi^-_{A,n\bar{n}}(k) \Bigg)^2 \Bigg] + \Bigg[\Bigg(\phi^+_{P,s\bar{s}}(k) + \frac{m_s}{E_s(k)} \phi^+_{A,s\bar{s}}(k) \Bigg)^2 - \Bigg(\phi^-_{P,s\bar{s}}(k) + \frac{m_s}{E_s(k)} \phi^-_{A,s\bar{s}}(k) \Bigg)^2 \Bigg] \Bigg\}, \tag{9.1}$$

where the various wave functions are those for the state *i*.

We calculate the singlet and octet decay constants in terms of the divergence of the currents

$$A^{(8)}_\mu(x) = \bar{q}(x)\gamma_\mu\gamma_5\lambda^8 q(x)/\sqrt{2} \tag{9.2}$$

and

$$A^{(0)}_\mu(x) = \bar{q}(x)\gamma_\mu\gamma_5\lambda^0 q(x)/\sqrt{2}. \tag{9.3}$$

We find

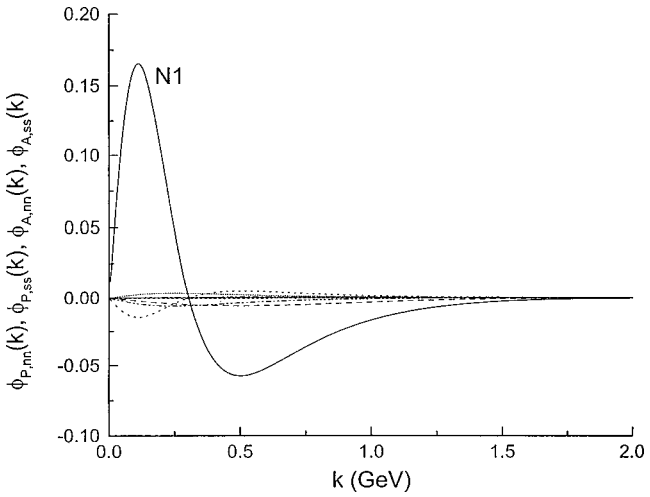

FIG. 11. The wave function of the $\eta(1440)$ found at 1411 MeV. (Symbols the same as in Fig. 8.)

$$\tilde{f}^{(8)}_{\eta,i}=\sqrt{\tfrac{2}{3}}\frac{n_c}{\pi^2}\frac{\sqrt{N_i}}{M_i}\int dk\,k\Bigg\{\left(\frac{m_u}{E_u(k)}\right)\times[\phi^+_{P,nn}(k)-\phi^-_{P,nn}(k)+\phi^+_{A,nn}(k)+\phi^-_{A,nn}(k)]-\left(\frac{m_s}{E_s(k)}\right)[\phi^+_{P,ss}(k)-\phi^-_{P,ss}(k)+\phi^+_{A,ss}(k)+\phi^-_{A,ss}(k)]\sqrt{2}\Bigg\} \tag{9.4}$$

and

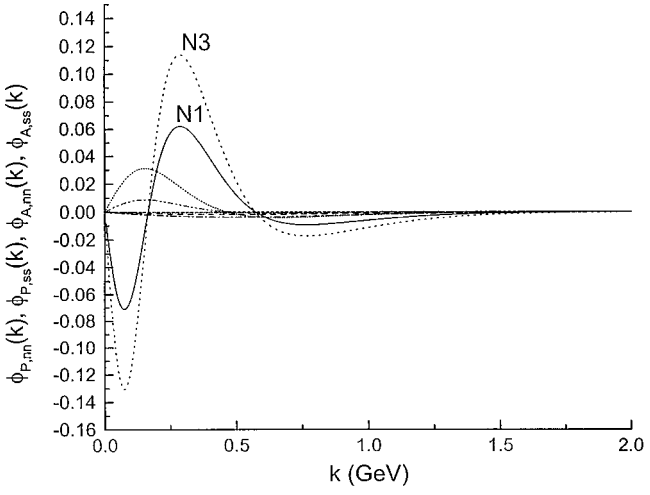

FIG. 12. The wave function of the state found at 1653 MeV in our calculation. (Symbols the same as in Fig. 8.)

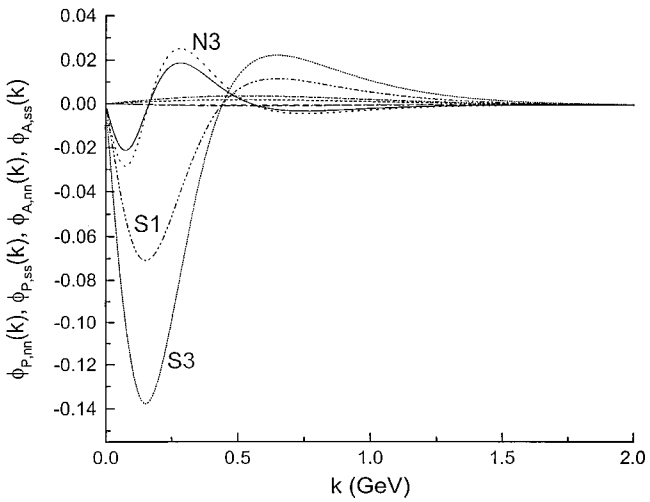

FIG. 13. The wave function of the state found at 1698 MeV in our calculation. (Symbols the same as in Fig. 8.)

$$\tilde{f}^{(0)}_{\eta,i}=\sqrt{\tfrac{2}{3}}\frac{n_c}{\pi^2}\frac{\sqrt{N_i}}{M_i}\int dk\,k\Bigg\{\left(\frac{m_u}{E_u(k)}\right)\times[\phi^+_{P,nn}(k)-\phi^-_{P,nn}(k)+\phi^+_{A,nn}(k)+\phi^-_{A,nn}(k)]\sqrt{2}+\left(\frac{m_s}{E_s(k)}\right)[\phi^+_{P,ss}(k)-\phi^-_{P,ss}(k)+\phi^+_{A,ss}(k)+\phi^-_{A,ss}(k)]\Bigg\}. \tag{9.5}$$

X. RESULTS OF NUMERICAL COMPUTATIONS

The parameters G_S and G_D appear in our Lagrangian. The parameters needed for a study of the eta mesons are G_{00}, G_{88}, and G_{08} [24]. For these mesons, we have

$$G_{00}=G_S+\frac{G_D}{2}C_{00}, \tag{10.1}$$

$$G_{88}=G_S+\frac{G_D}{2}C_{88}, \tag{10.2}$$

and

$$G_{08}=\frac{G_D}{2}C_{08}, \tag{10.3}$$

where

$$C_{00}=-\frac{2}{3}(2\langle\bar{u}u\rangle+\langle\bar{s}s\rangle), \tag{10.4}$$

$$C_{88}=-\frac{1}{3}(\langle\bar{s}s\rangle-4\langle\bar{u}u\rangle), \tag{10.5}$$

and

TABLE II. Parameters used for the calculations reported upon in Table I.

	Set I	Set II	Set III	Set IV
G_S (GeV^{-2})	11.84	11.84	11.84	11.57
G_D (GeV^{-5})	−180.0	−200.0	−220.0	−161.6
G_V (GeV^{-2})	13.00	13.00	13.00	13.00
m_u (GeV)	0.364	0.364	0.364	0.364
m_s (GeV)	0.585	0.585	0.585	0.585
G_{00} (GeV^{-2})	8.465	8.090	7.715	8.54
G_{88} (GeV^{-2})	12.90	13.02	13.13	12.52
G_{08} (GeV^{-2})	−0.4458	−0.4953	−0.5483	0

$$C_{08}=\frac{\sqrt{2}}{3}(\langle\bar{u}u\rangle-\langle\bar{s}s\rangle). \tag{10.6}$$

We take $\langle\bar{s}s\rangle/\langle\bar{u}u\rangle=1.689$, as determined in Ref. [25]. We also put $\langle\bar{u}u\rangle=-(0.248\ \text{GeV})^3=-0.01525\ \text{GeV}^3$ and obtain $C_{00}=0.03750\ \text{GeV}^3$, $C_{88}=-0.01175\ \text{GeV}^3$, and $C_{08}=-0.01214\ \text{GeV}^3$. We remark that $\langle\bar{u}u\rangle$ appears multiplied by G_D, so that the relevant parameter is the product of these quantities. (See the Appendix.)

We have calculated $\tilde{f}_\eta^{(8)}$, $\tilde{f}_\eta^{(0)}$, $\tilde{f}_{\eta'}^{(8)}$, and $\tilde{f}_{\eta'}^{(0)}$ using the expressions given in Sec. IX. The definitions of other decay constants and mixing angles were given in the Introduction. Our results are shown in Table I, where comparison is made with the parameters that were determined in Ref. [12] using experimental data. We note that the results for set IV are not consistent, since we have put $G_{08}=0$, even though we have $G_D=-166.6\ \text{GeV}^{-5}$. (See Table II.) As can be seen from Table I, the values of θ_η and $\theta_{\eta'}$ (or θ_0 and θ_8) are too large when we use the parameters of set IV. We have presented these results, however, since we are interested in demonstrating how a proper treatment of the singlet-octet mixing indicated by the 't Hooft interaction yields quite good results.

To clarify the observation, we see that inspection of Eqs. (7.17) and (7.18) shows that the mixing between $\phi^+_{P,0}(k)$ and $\phi^+_{P,8}(k)$ depends upon the quantity $E_{08}(k)\,\delta(k-k')+G_{08}H^{PP}_{88}(k,k')$ or, equivalently, $E_{80}(k)\,\delta(k-k')+G_{80}H^{PP}_{00}(k,k')$. From Eq. (7.16) we see that $E_{08}(k)=E_{80}(k)$ is negative. We note that $G_{08}=G_{80}$ is also negative, as are $H^{PP}_{88}(k,k')$ and $H^{PP}_{00}(k,k')$. [See the Appendix, where we may see that $H^{PP}_{88}(k,k')=H^{PP}_{00}(k,k')$.] Therefore, the inclusion of the 't Hooft interaction reduces the mixing induced by the presence of $E_{08}(k)$, since $G_{08}H^{PP}_{88}(k,k')$ is positive. That feature may be seen in the results given in Table I. For example, let us consider the results of parameter set IV. We see that if we put $G_{08}=0$, we have $\theta_0=-19.4°$ and $\theta_8=-32.8°$, which are significantly larger in magnitude than the values of θ_0 and θ_8 obtained from fits to empirical data, or from theoretical analysis. However, if we make a more consistent calculation with finite values of G_{08} (see Tables II and III), the values of θ_0 and θ_8 are brought into agreement with the theoretical or empirical values [12]. (The values of $G_D=-180$, -200, or $-220\ \text{GeV}^{-5}$ correspond to generally suggested values of that parameters. For example, in Ref. [24] we find the choice $G_D=-185\ \text{GeV}^{-5}$.)

TABLE III. The first column shows the expressions for the various pseudoscalar coupling taken from Ref. [24]. We use $G_S=11.84\ \text{GeV}^{-2}$, $G_D=-200\ \text{GeV}^{-5}$, $\alpha=-0.01524\ \text{GeV}^3$, and $\gamma=-0.02575\ \text{GeV}^3$ to obtain the values in the second column. (See set II of Table II.)

Effective pseudoscalar coupling constants [24]	G_{00}, G_{08}, and G_{88} (GeV^{-2})
$G_{00}=G_S-\frac{G_D}{3}(\alpha+\beta+\gamma)$	$11.84-3.75=8.09$
$G_{88}=G_S-\frac{G_D}{6}(\gamma-2\alpha-2\beta)$	$11.84+1.17=13.01$
$G_{08}=-\frac{\sqrt{2}}{12}G_D(2\gamma-\beta-\alpha)$	-0.4953

In Table I we have compared our values with those obtained from an analysis of experimental data [12]. We may also make contact with the theoretical results of extended chiral perturbation theory and other studies. For example, in Table I of Ref. [14] we find that $\theta_8=-21.0°$ and $\theta_0=-2.7°$ for the theoretical scheme put forth in Ref. [13]. For the phenomenological scheme of Ref. [13], the values given are $\theta_8=-21.2°$ and $\theta_0=-9.2°$. We see that the calculated values presented in our Table I for θ_8 and θ_0 are in closer correspondence with the phenomenological scheme of Ref. [13] than with the theoretical scheme. In addition, we note that extended chiral perturbation theory gives $\theta_8\simeq-20.5°$ and $\theta_0\simeq4°$ [7,8]. The values of $\theta_0-\theta_8$ obtained from our values of θ_8 and θ_0 are also consistent with the value of $\theta_0-\theta_8=-16.4°$ calculated in Ref. [10] by a somewhat different theoretical method than that used in Refs. [7], [8]. We see that the values obtained using chiral perturbation theory for $\theta_0-\theta_8$ are quite close to the values of $-15.6°$ or $-16.6°$ given in our Table I for $G_D=-180$ and $-200\ \text{GeV}^{-5}$, respectively.

XI. DISCUSSION

In the absence of a confining interaction, the NJL model does not allow for a description of radially excited states. The model leads to a separable interaction in each channel such that the vertex function is proportional to the regulator. [See Eqs. (5.1) and (5.12).] To deal with this problem, Volkov and collaborators have introduced additional separable interactions in each channel. These new terms allow for a description of radially excited states [26–28]. More closely related to our work are the results described in Refs. [29–32]. In Refs. [29,30] the authors include a confinement model that has scalar, pseudoscalar, and vector confining interactions. They solve the Bethe-Salpeter equation and describe a large number of light meson states. However, they do not include pseudoscalar–axial-vector coupling in their formalism. Other work related to ours may be found in Ref. [33], where meson spectra are calculated using many-body techniques based upon the RPA. That work is part of a comprehensive program to investigate hadron structure using an

effective Lagrangian obtained from QCD [34].

In the present work we have shown how to derive relativistic RPA equations that may be used to calculate the properties of radially excited states of pseudoscalar mesons. The RPA representation of the wave function components is seen to be particularly well suited if one wishes to provide a physical description of the states in terms of their $n\bar{n}$ or $s\bar{s}$ components. It is also easy to see the relative importance of the γ_5 and $\gamma_0\gamma_5$ vertices. It is worth noting that the deviations from ideal mixing are due to the presence of the 't Hooft interaction. We find that $n\bar{n}$-$s\bar{s}$ mixing is most important for the $\eta(547)$ and $\eta'(958)$. The other states are mainly either $n\bar{n}$ or $s\bar{s}$ states.

In this work we have demonstrated that the 't Hooft interaction exhibits two important features. [That interaction breaks the $U_A(1)$ symmetry that the Lagrangian would have in the limit of zero current quark masses and reduces the number of Goldstone bosons from nine to eight.]

The first feature that has been emphasized in applications of the NJL model is the fact that one may fit the energies of the $\eta(547)$ and $\eta'(958)$, if the strength of the 't Hooft interaction is chosen appropriately. The second feature that we describe in this work has not been noted previously. We have found that the singlet-octet coupling induced by the 't Hooft interaction, which is proportional to the parameter G_{08}, is of the correct magnitude to compensate for the singlet-octet coupling introduced by function $E_{08}(k)$, such as to bring the values of the mixing angles into the range specified by extended chiral perturbation theory ($\theta_0 \simeq 4°$, $\theta_8 \simeq -20°$ [7,8]) or by fits to experimental data [12,14].

Ideally, we would like to maintain chiral symmetry and covariance in our generalized NJL model. We have emphasized covariance in our work, rather than symmetry. That leads to some problems in the description of the radial excitations of the pion [35]. However, our description of the eta mesons including the radially excited states is quite satisfactory, indicating that chiral symmetry constraints may be less important than the covariance of the formalism and a proper treatment of pseudoscalar–axial-vector coupling. Finally, we note that one may consult Ref. [36] for an extensive discussion of large n_c in chiral perturbation theory.

APPENDIX

In this appendix we define the various interaction elements needed to construct the eight equations given as Eqs. (7.17)–(7.24). We begin by working in the $n\bar{n}$-$s\bar{s}$ representation and first consider the $n\bar{n}$ space. Then we have

$$H_{n\bar{n}}^{PP}(k,k') = -\frac{2n_c}{\pi^2} kk' e^{-k^2/2\alpha^2} e^{-k'^2/2\alpha^2}, \tag{A1}$$

$$H_{n\bar{n}}^{PA}(k,k') = -\frac{2n_c}{\pi^2} kk' e^{-k^2/2\alpha^2} e^{-k'^2/2\alpha^2}, \tag{A2}$$

$$H_{n\bar{n}}^{AP}(k,k') = H_{n\bar{n}}^{PA}(k,k'), \tag{A3}$$

$$H_{n\bar{n}}^{AA}(k,k') = \frac{n_c}{\pi^2} \frac{2m_u}{E_u(k)} kk' e^{-k^2/2\alpha^2} e^{-k'^2/2\alpha^2}, \tag{A4}$$

$$H_{n\bar{n}}^{PP(C)}(k,k') = -\frac{1}{\pi^2} kk' \frac{[m_u^2 - E_u(k)E_u(k')]V_0(k,k')}{E_u(k)E_u(k')}, \tag{A5}$$

and

$$H_{n\bar{n}}^{AA(C)}(k,k') = H_{n\bar{n}}^{PP(C)}(k,k'). \tag{A6}$$

Here, with $x = \cos\theta$,

$$V_0(k,k') = \frac{1}{2}\int_{-1}^{1} dx\, V^C(\vec{k}-\vec{k}'). \tag{A7}$$

The various elements, such as $H_{s\bar{s}}^{PP}(k,k')$, are obtained by replacing m_u and $E_u(k)$ with m_s and $E_s(k)$ in the equations presented above.

We may then define

$$H_{00}^{PP}(k,k') = \frac{1}{3}[2H_{n\bar{n}}^{PP}(k,k') + H_{s\bar{s}}^{PP}(k,k')], \tag{A8}$$

$$H_{08}^{PP}(k,k') = \frac{\sqrt{2}}{3}[H_{n\bar{n}}^{PP}(k,k') - H_{s\bar{s}}^{PP}(k,k')], \tag{A9}$$

and

$$H_{88}^{PP}(k,k') = \frac{1}{3}[H_{n\bar{n}}^{PP}(k,k') + 2H_{s\bar{s}}^{PP}(k,k')], \tag{A10}$$

with $H_{80}^{PP}(k,k') = H_{08}^{PP}(k,k')$. Values for the other interaction terms in Eqs. (7.17)–(7.24) may be found by using relations of the form given in Eqs. (A8)–(A10). We see that $H_{00}^{PP}(k,k') = H_{88}^{PP}(k,k')$ and that $H_{08}^{PP}(k,k') = 0$.

[1] F. J. Gilman and R. Kauffman, Phys. Rev. D **36**, 2761 (1987).
[2] A. Bramon and M. D. Scadron, Phys. Lett. B **234**, 346 (1990).
[3] P. Ball, J.-M. Frère, and M. Tytgat, Phys. Lett. B **365**, 367 (1996).
[4] A. Bramon, R. Escribano, and M. D. Scadron, Phys. Lett. B **403**, 339 (1997).
[5] A. Bramon, R. Escribano, and M. D. Scadron, Eur. Phys. J. C **7**, 271 (1999).
[6] E. P. Venagopal and B. R. Holstein, Phys. Rev. D **57**, 4397 (1998).
[7] H. Leutwyler, Nucl. Phys. B (Proc. Suppl.) **64**, 223 (1998).
[8] R. Kaiser and H. Leutwyler, hep-ph/9806336.
[9] P. Herrera-Silkody, J. I. Latorre, P. Pascual, and J. Jaron, Nucl. Phys. **B497**, 345 (1997).
[10] N. Beisert and B. Borasoy, Eur. Phys. J. A **11**, 329 (2001).
[11] T. Feldman and P. Kroll, Eur. Phys. J. C **5**, 327 (1998).

[12] R. Escribano and J.-M. Frère, Phys. Lett. B **459**, 288 (1999).
[13] Th. Feldman, P. Kroll, and B. Stech, Phys. Rev. D **58**, 114006 (1998).
[14] Th. Feldman, P. Kroll, and B. Stech, Phys. Lett. B **449**, 339 (1999).
[15] L. S. Celenza, Bo Huang, Huangsheng Wang, and C. M. Shakin, Phys. Rev. C **60**, 025202 (1999); **60**, 039901(E) (1999).
[16] L. S. Celenza, Bo Huang, Huangsheng Wang, and C. M. Shakin, Phys. Rev. C **60**, 035206 (1999).
[17] L. S. Celenza, Bo Huang, Huangsheng Wang, and C. M. Shakin, Phys. Rev. C **60**, 065209 (1999); **60**, 065210 (1999).
[18] L. S. Celenza, Shun-Fun Gao, Bo Huang, Huangsheng Wang, and C. M. Shakin, Phys. Rev. C **61**, 035201 (2000).
[19] C. M. Shakin and Huangsheng Wang, Phys. Rev. D **63**, 014019 (2001); **63**, 074017 (2001); **63**, 114007 (2001).
[20] L. S. Celenza, Huangsheng Wang, and C. M. Shakin, Phys. Rev. C **63**, 025209 (2001).
[21] L. S. Celenza, Xiang-Dong Li, and C. M. Shakin, Phys. Rev. C **55**, 1492 (1997).
[22] A. L. Fetter and J. D. Walecka, *Quantum Theory of Many-Particle Systems* (McGraw-Hill, New York, 1971), Chap. 15.
[23] D. J. Rowe, *Nuclear Collective Motion: Models and Theory* (Methuen, London, 1970), Fig. 14.3.
[24] T. Hatsuda and T. Kunihiro, Phys. Rep. **247**, 221 (1994).
[25] G. Amoros, J. Bijnens, and P. Talavera, Nucl. Phys. **B602**, 87 (2001).
[26] M. K. Volkov and V. L. Yudichev, Phys. Part. Nucl. **31**, 282 (2000).
[27] M. K. Volkov and V. L. Yudichev, Int. J. Mod. Phys. A **14**, 4621 (1999).
[28] M. K. Volkov, D. Ebert, and M. Nagy, Int. J. Mod. Phys. A **13**, 5443 (1998).
[29] R. Ricken, M. Koll, D. Merten, B. Metsch, and H. R. Petry, Eur. Phys. J. A **9**, 221 (2000).
[30] M. Koll, R. Ricken, D. Merten, B. Metsch, and H. Petry, Eur. Phys. J. A **9**, 73 (2000).
[31] B. Metsch and H. R. Petry, Acta Phys. Pol. B **27**, 3307 (1996).
[32] C. R. Münz, J. Resay, B. C. Metsch, and H. R. Petry, Nucl. Phys. **A578**, 418 (1994).
[33] F. J. Llanes-Estrada and S. R. Cotanch, Phys. Rev. Lett. **84**, 1102 (2000).
[34] S. R. Cotanch and F. J. Llanes-Estrada, to appear in Proceedings for Confinement IV, Vienna, 2000, hep-ph/0009191.
[35] C. M. Shakin and Huangsheng Wang, Brooklyn College Report No. BCCNT:01/081/306 (2001).
[36] B. Kaiser and H. Leutwyler, Eur. Phys. J. C **17**, 623 (2000).